Deep Geoelectrical Soundings at Camp Roberts Sanitary Landfill, San Luis Obispo County, California

Les P. Beard
Environmental Sciences Division
Oak Ridge National Laboratory
Oak Ridge, Tennessee

Prepared for:

Wayne A. Mandell
U.S. Army Environmental Center
Aberdeen Proving Ground, Maryland

December 5, 2001

Table of Contents

1. Introduction …….. 1
2. Method descriptions ……. 1
   2.1 CSAMT sounding ……..…..…… 1
   2.2 TEM central loop sounding ……...…… 3
3. Site description …….……..…… 3
4. Data collection ……...…… 4
   4.1 CSAMT Data ……..... 6
   4.2 TEM Data ……..……...…… 7
5. Data reduction and interpretation …….…….. 7
   5.1 CSAMT Data ……...… 7
   5.2 TEM Data ……..……. 15
6. Discussion and Conclusions ……..…….……...… 16
7. Recommendations ……...…….. 18
8. Acknowledgments ……..…… 19
9. References ……..…… 19
10. Appendix I ……..…… 21
11. Appendix II ……..…….. 31

List of Figures

Figure 1.	**CSAMT transmitter and receiver…….**	**2**
Figure 2.	**TEM transmitter and receiver……..**	**4**
Figure 3.	**Landfill site map with sounding locations……**	**5**
Figure 4.	**CSAMT apparent resistivity, E_x/H_y, Line 1…….**	**9**
Figure 5.	**CSAMT Bostick resistivity, E_x/H_y, Line 1……**	**9**
Figure 6.	**Tomographic 2-D seismic velocity inversion ……..…….**	**10**
Figure 7.	**CSAMT apparent resistivity, E_y/H_x, Line 1…….**	**11**
Figure 8.	**CSAMT Bostick resistivity, E_y/H_x, Line 1……**	**11**
Figure 9.	**CSAMT apparent resistivity, E_x/H_y, Line 2…….**	**12**
Figure 10.	**CSAMT Bostick resistivity, E_x/H_y, Line 2……**	**12**
Figure 11.	**CSAMT apparent resistivity, E_y/H_x, Line 2…….**	**13**
Figure 12.	**CSAMT Bostick resistivity, E_y/H_x, Line 2……**	**13**
Figure 13.	**Groundwater table as mapped from boreholes ….……**	**14**
Figure 14.	**TEM apparent resistivity and 1-D inversion, site 5……**	**16**

List of Tables

Table 1. GPS positions of CSAMT transmitters and receivers and TEM receivers……	**6**

EXECUTIVE SUMMARY

In October, 2001, two different electromagnetic deep sounding methods were employed at the sanitary landfill in Camp Roberts, California. The objective of the investigation was to assess geological and hydrological conditions at depths beyond those of previous borehole explorations and geophysical investigations. The methods used were the controlled source audiomagnetotelluric method (CSAMT) and the central loop transient electromagnetic sounding method (TEM). The depth of investigation for both methods was about 300 m, varying somewhat with the electrical character at each sounding site. The Camp Roberts sanitary landfill is a low noise environment, well suited for deep electromagnetic sounding.

Both methods indicate a high conductivity layer at a depth of about 200 m. This may be a layer containing saline water, possibly the top of the Pancho Rico formation, a marine sedimentary unit. Both methods indicate a sub-horizontally layered section with a gradual increase in electrical conductivity with depth from the surface to about 100 m, probably indicative of increasing moisture content with increasing depth.

Although the TEM soundings showed the first conductivity decrease at depths roughly corresponding to the previously mapped groundwater table, it is not unambiguously imaged by either the TEM or the CSAMT method. If in previous investigations the water table was mapped correctly throughout the survey area, then the lack of resolution probably implies groundwater uncontaminated by large amounts of electrically conductive contaminants. Alternatively, the groundwater table, as previously recorded, could be mapping discontinuous perched water and thin aquifers, both of which are likely to exist in an alluvial environment.

TEM soundings show a thin, highly conductive layer at about 100 m depth. The conductivity of the layer is sufficiently high that it is most likely of natural origin, the most likely candidate being saline pore fluids. The layer is consistent on 7 of 8 TEM soundings. CSAMT inversions also show a zone of higher conductivity near 100 m depth, but the resistivity contrast is not so pronounced in the CSAMT inversion, and the conductive zone appears much thicker.

CSAMT data show an irregular conductive unit, possibly a confined aquifer, at a depth of about 60 m in Line 1. The unit bifurcates and disappears toward the north end of Line 1, and grows thicker to the south, becoming indistinguishable from a deeper conductor in this part of the line. CSAMT data on the north end of Line 1 show a conductive zone at about 250 m depth. This zone shallows abruptly near the south end of the line to a depth of 200 m. A similar step is seen in a seismic velocity from a line paralleling Line 1. CSAMT data on Line 2 show a conductive zone, shallower near the center of the line than at either end, consistent with the current groundwater table map that shows shallower groundwater depth in the same area.

1 INTRODUCTION

During October 1-5, 2001, deep geo-electromagnetic sounding data were collected at the Camp Roberts Sanitary Landfill, San Luis Obispo County, California. The geophysical methods used were the controlled source audiomagnetotelluric method (CSAMT) and the central loop transient electromagnetic sounding (TEM) method. The objective of the survey was to obtain hydrological and geological information at subsurface depths of up to 300 m, deeper than existing wells and boreholes in the area, and deeper than has been imaged in previous geophysical investigations (Doll et al., 2000). Bedrock depths have not been determined by drilling, and the CSAMT and TEM sounding methods offer the possibility of detecting well-consolidated units provided the electrical contrast between consolidated units and overlying sediments is adequate. Information on depth to the groundwater table may also be derived from CSAMT and TEM soundings given sufficient electrical contrast. Both methods respond to thick electrically conductive zones, without regard to the source of conductivity, making interpretation based strictly on electromagnetic data ambiguous.

2 METHOD DESCRIPTIONS

2.1 CSAMT sounding

The CSAMT sounding method is a variant on the magnetotelluric method (MT). MT uses naturally produced electromagnetic fields that can be used to probe to depths of several tens of kilometers. The depth of investigation is a function of frequency. Low frequencies probe deeper than high frequencies. High frequencies—up to 100 000 Hz—are necessary for shallow depth soundings, but some high frequency components have low natural source intensities and must be enhanced using an artificial source. With the STRATAGEM EH-4 system (Geometrics, 2000) used at Camp Roberts, a controlled source was used to produce signals down to frequencies of about 800 Hz. Below 800 Hz, natural audiomagnetotelluric signals were sufficiently strong to provide the source. The lowest frequency recorded was 12 Hz.

The STRATAGEM transmitter and receiver are illustrated in Figure 1. The receiver consists of two orthogonal grounded wires to detect the electric fields in the survey line direction and at right angles to it. Aligned parallel to the wires are two cylindrical wire coils that record magnetic field strength. For each frequency *f*, the apparent resistivity of the earth can be determined using the relation

$$\rho_x = \frac{1}{2\pi f \mu} \left| \frac{E_x}{H_y} \right|^2 \text{ ohm-m}$$

where μ is the magnetic permeability of the earth, E_x is the electric field measured in the direction of the profile line, and H_y is the magnetic field intensity in the direction

perpendicular to profile. A similar expression for ρ_y applies for measurements of E_y and H_x. Over a horizontally layered, isotropic earth, $\rho_y = \rho_x$.

The STRATAGEM transmitter produces a moment of 400 A-m^2 at frequencies ranging from 64 000 Hz to 800 Hz. The transmitter is typically set up 200-300 meters off the profile line, far enough from the receiver that for frequencies down to 800 Hz the transmitted wave can be considered far-field. Far-field EM data can be treated with computationally simple plane wave magnetotelluric analysis tools.

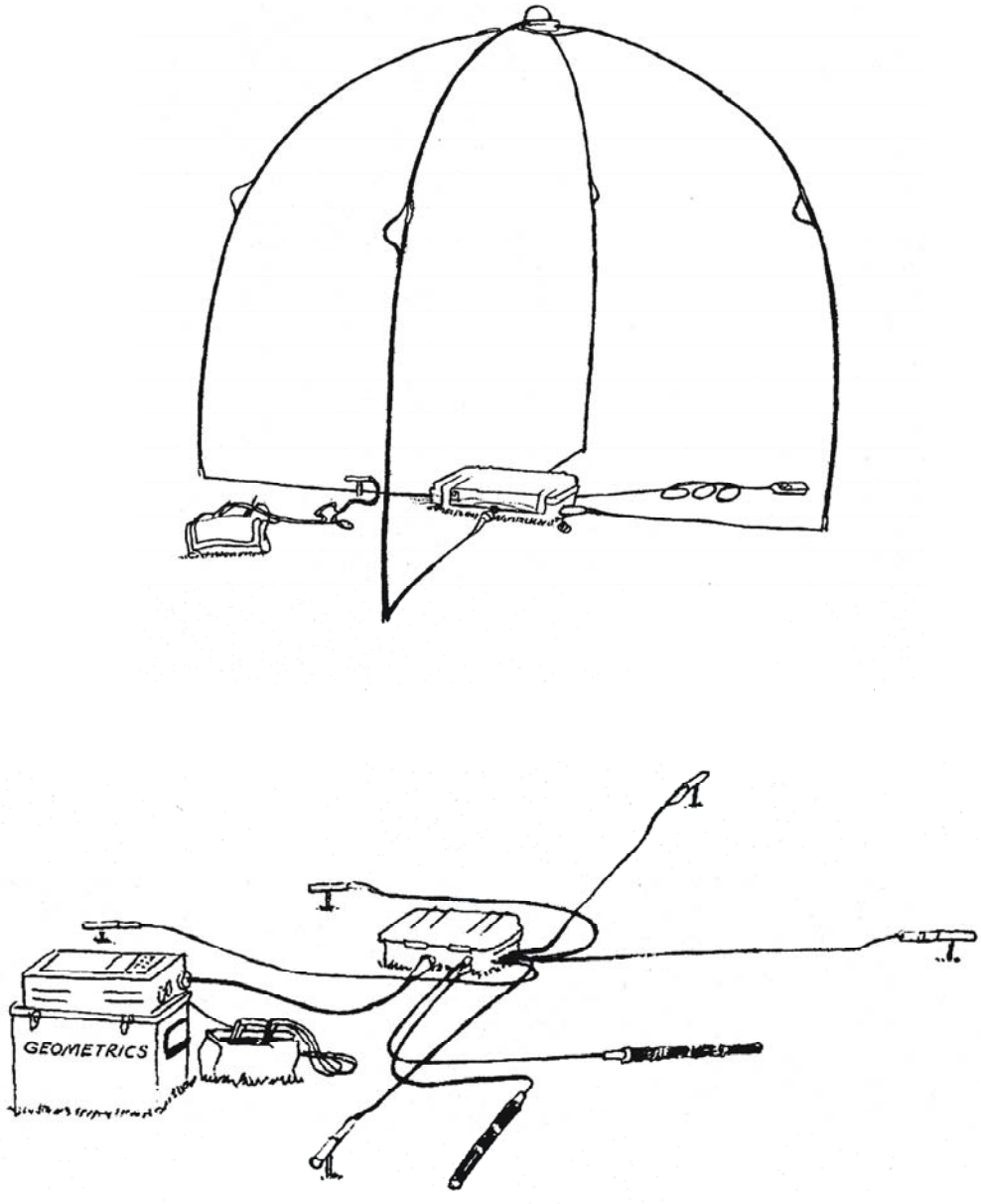

Figure 1. Geometrics STRATAGEM EH-4 transmitter (top) and receiver (bottom). Receiver setup consists of x- and y-directed grounded electric field dipoles and x- and y-directed magnetic field sensors. A grounding electrode maintains proper voltage levels. (Adapted from Geometrics, 2000.)

2.2 TEM central loop sounding

Whereas CSAMT measurements are made at discrete frequencies while the electrical source—natural or artificial—is applied, TEM measurements are taken over a range of time after an exciting source loop is turned off. Once switched off, the current loop at the earth's surface induces currents in the earth. These currents diffuse downward into the earth in much the same manner as a smoke ring spreads through the air. Their decay is rapid, and is typically measured by the time rate of change of the vertical component of the magnetic field in a sensor set up at the center of a large diameter wire loop. The decay with time of the field is proportional to the conductivity of the earth with the decay being more gradual over a more conductive earth.

The TEM equipment used at Camp Roberts was a Geonics TEM 57 transmitter (Figure 2) powered by a gasoline-powered generator that sent 15 amperes of electrical current through a 100 m x 100 m square loop. A Geonics Protem receiver coil (Figure 2), placed in the center of the square transmitter loop, measured the time rate of decay of the magnetic field $\partial B_z / \partial t$ over 20 time gates. The first gate begins at 80 μs and the last gate ends at 782 μs, covering depths from a few tens to a few hundred meters.

3 SITE DESCRIPTION

The Camp Roberts Sanitary Landfill appears to be relatively well suited for deep geoelectrical prospecting methods. Other than the presence of metallic landfill debris and some grounded metal fences, there was little indication of noise sources that could adversely affect the data, e.g. power lines, energized underground cables, or networks of pipes. Topographic relief is modest, as can be seen in Figure 3. Dip of bedding is shallow, 10° or less where recorded in drilling logs (Geosystem Consultants, 1995). The geological section examined in previous investigations consists entirely or almost entirely of a single formation, the Paso Robles. The Paso Robles Formation is a non-marine alluvial formation consisting of relatively impermeable claystones, siltstones, and silty sandstones interfingered with more permeable sandstones and conglomerates. The complexity of the interfingered sub-units in the Paso Robles Formation implies the probable presence of perched water tables and confined aquifers. Geosystem Consultants reports total dissolved solids in wells in the vicinity of the geolectrical soundings to be about 400 ppm. If the solid constituent is entirely NaCl, this level translates to a water resistivity on the order of 1 ohm-m (Keller, 1988). This in turn translates to formation resistivities on the order of 10 ohm-m in reasonably porous sandstones and conglomerates. The Paso Robles Formation overlies the Pancho Rico Formation, a formation of clastic units similar to the Paso Robles Formation, but one having a marine origin. The depth to the top of the Pancho Rico is unknown in the area of the landfill, but is at least deeper than the deepest borehole, MW-3, which bottoms at about 100 m depth.

Figure 2. Geonics TEM sounding system. Top panel shows transmitter console. A gasoline powered generator supplies power to the transmitter sufficient to send a 15 A current through a 100 m x 100 m square transmitter loop. Bottom panel shows PROTEM receiver console and receiver coil. The receiver coil is located at the center of the 100 m x 100 m transmitter loop.

4 DATA COLLECTION

CSAMT and TEM data were collected along the two lines shown in Figure 3. The line positions were chosen to pass through magnetically quiet areas of the landfill, as assessed from a previous magnetic survey over the area (Figure 6 in Doll et al., 2000). The line directions were chosen so that they would be sub-parallel to two seismic refraction lines (Doll et al., 2000). Receiver positions were recorded using a hand-held GPS receiver accurate to about +/-5 meters. CSAMT transmitter locations were also recorded. These are listed in Table 1.

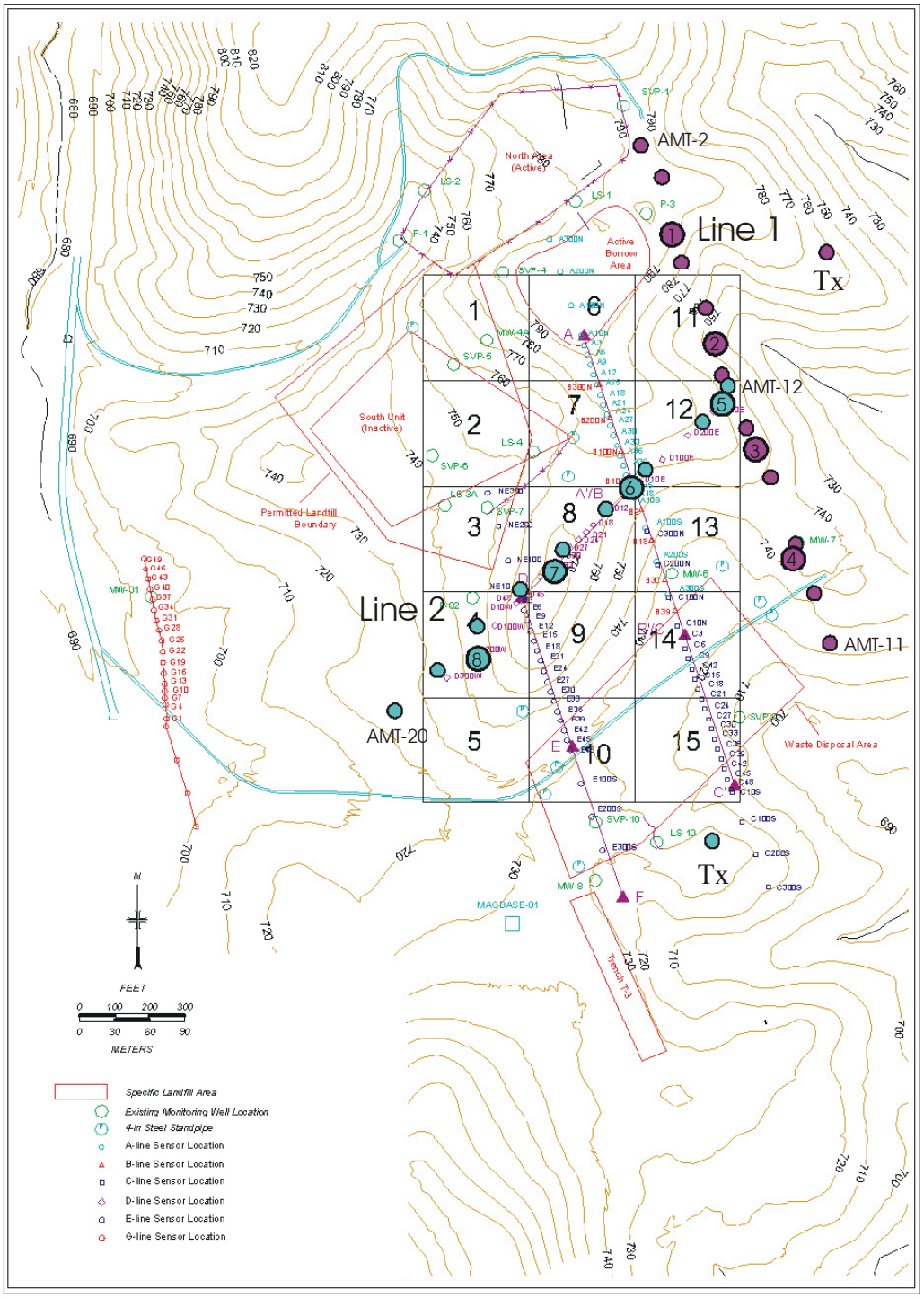

Figure 3. Landfill site map showing the CSAMT and TEM sounding locations on top of previous geophysical surveys. CSAMT sites: small circles, TEM sites: large circles. Line 1: magenta circles. Line 2: light blue circles. Two circles labeled Tx set well off either line represent CSAMT transmitter sites. (Modified from Figure 1, Doll et al., 2000).

Table 1. GPS positions of CSAMT transmitter and receiver stations and TEM receiver stations.

Line number	Position along profile (m)	Latitude (d m s.s)	Longitude (d m s.s)	Comment
AMT 1	0	35 46 33.6	120 43 59.0	40 m N of well P-3
AMT 1	50	35 46 32.7	120 43 58.3	
AMT 1	100	35 46 30.3	120 43 57.7	
AMT 1	150	35 46 29.0	120 43 56.9	
AMT 1	200	35 46 27.1	120 43 56.4	
AMT 1	250	35 46 25.6	120 43 55.6	
AMT 1	300	35 46 24.2	120 43 54.8	
AMT 1	350	35 46 22.3	120 43 54.0	3 m W of well MW-7
AMT 1	400	35 46 20.9	120 43 53.4	
AMT 1	450	35 46 19.5	120 43 52.9	
AMT 1	Transmitter	35 46 30.5	120 43 52.7	
AMT 2	0	35 46 26.8	120 43 56.2	
AMT 2	50	35 46 25.8	120 43 57.1	
AMT 2	100	35 46 24.5	120 43 59.1	
AMT 2	150	35 46 23.4	120 44 00.5	
AMT 2	200	35 46 22.3	120 44 02.0	
AMT 2	250	35 46 21.2	120 44 03.5	
AMT 2	300	35 46 20.2	120 44 05.0	
AMT 2	350	35 46 19.0	120 44 06.4	
AMT 2	400	35 46 17.9	120 44 07.9	
AMT 2	Transmitter	35 46 14.0	120 43 57.1	
TEM 1	0	35 46 31.1	120 43 58.0	
TEM 1	100	35 46 28.0	120 43 56.6	
TEM 1	200	35 46 25.0	120 43 55.3	
TEM 1	300	35 46 21.9	120 43 54.1	
TEM 2	0	35 46 26.3	120 43 56.4	
TEM 2	100	35 46 24.0	120 43 59.6	
TEM 2	200	35 46 21.7	120 44 02.3	
TEM 2	300	35 46 19.3	120 44 05.0	

4.1 CSAMT Data

CSAMT receiver and transmitter positions are shown in Figure 3. Line 1 followed a heading of 160° (clockwise from true north) with the center of the receiver array located about 40 m north of well P-3. After the STRATAGEM collected a time series of duration sufficient for processing over a frequency band from 64 000 Hz to 12 Hz, usually 15-30 minutes, the receiver array was moved 50 m down the line. The total time required for moving the receiver, setting it up, and data collection was about 45 minutes. Line 1 consisted of 10 receiver positions—AMT-2 throuth AMT-11—along a 450 m long line. The 8th receiver position, at x = 350 m, is located 3 m west of well MW-7. Line 2,

having 9 receiver locations, began with AMT-12 at about the halfway mark along Line 1 and continued 400 m along a 225° heading with a station spacing of 50 m, ending with station AMT-20. Noise levels were low, increasing at the lowest frequencies because low frequency data can be stacked fewer times than high frequency data for a given time series.

4.2 TEM Data

Transient EM data were collected along the same two lines where the CSAMT data were collected, but a wider station spacing was used because of the size of the transmitter loop (100 m x 100 m). Data were collected using the central loop configuration in which a receiver coil is located at the center of a 100 m x 100 m square transmitter loop. A current of 15 A was passed through the loop using a gasoline generator powered Geonics EM-57 transmitter and then abruptly turned off. The decaying magnetic field was measured using a Protem digital receiver system. Three separate decay curves were recorded at each site. Four soundings sites spaced 100 m apart were collected along each line. The first sounding receiver site on Line 2 (TEM-0005 in Appendix B) is also on Line 1, so Line 1 effectively has five TEM stations. Signal-to-noise was high on all gates except the latest time gate (gate 20).

5 DATA REDUCTION AND INTERPRETATION

5.1 CSAMT Data

CSAMT sounding data at each receiver location are shown in Appendix A. Line 1 consists of stations 2 (x = 0 m) through 11 (x = 450 m). Stations 12 (x = 0 m) through 20 (x = 400 m) are on Line 2. Each sounding shows records of apparent resistivity, phase, coherence, and 'true' resistivity as a function of depth computed from the Bostick relation (Bostick, 1977). These quantities are computed for electrical receivers oriented along the profile direction (the x-direction) and electrical receivers orthogonal to profile (the y-direction). Error bars on each of the data points show that the noise levels were in general low.

The Bostick resistivity is computed as a function of depth in the following manner. For a given frequency f there is an associated period T where $T = 1/f$. From T a penetration depth h is computed using the expression

$$h = \sqrt{\frac{\rho_a(T)T}{2\pi\mu_0}}$$

where $\rho_a(T)$ is the measured apparent resistivity at period T and μ_0 is the magnetic permeability of free space. The Bostick resistivity $\rho_B(h)$ is then computed from the equation

$$\rho_B(h) = \rho_a(T)\frac{1+m(T)}{1-m(T)}$$

where $m(T)$ is the slope of the apparent resistivity curve at period T as plotted on a log-log scale.

At each of the 19 sounding sites, the apparent resistivity curve as measured from the x-directed electric sensor is nearly coincident with the apparent resistivity curve from the y-directed electric sensor. In the presence of strong anisotropy or significant 2-D or 3-D structures, the curves can be expected to diverge. Their coincidence can be taken as strong evidence that a 1-D interpretation is valid.

Figure 4 shows apparent resistivity versus frequency for the x-directed electrical receivers (and y-directed magnetic sensors) along Line 1. These apparent resistivities translate to the resistivity-depth section using the Bostick relation shown above. Figure 5 shows a relatively conductive layer of about 10 ohm-m at a depth of about 70 m. This conductive zone is 0-50 m thick along the northern half of Line 1, and then gives way to deeper more resistive units until at a depth greater than 200 m another conductive unit is encountered. This lower conductive unit appears to occur at increasingly shallow depths toward the southern half of Line 1. The intermediate resistive unit does not occur in the last 4 stations of Line 1 (300-450 in Figure 5). Seismic data collected along a line sub-parallel to this line (Doll et al., 2001) show a high velocity zone that is shallow in the south and deepens to the north, a structure similar to but shallower than the deep EM conductive zone. Figure 6 shows a 2-D velocity inversion along seismic lines parallel to CSAMT Line 1. The seismic line in Figure 6 is about 275 m long and from the point denoted A/B' in Figure 3, coincident with TEM site 6, extends southward to the point marked C' near the southeast corner of Block 15.

Figure 7 shows the apparent resistivity map for the y-directed electrical receivers. The amplitude and pattern of response is very similar to Figure 4, indicating a horizontally layered earth is a reasonable approximation. The Bostick resistivity section shown in Figure 8 is similar to Figure 5, except on the south end of the line the resistivities are higher, and the shallowing to the south of the deep conductor does not occur.

Figures 9 and 10 show apparent resistivities and Bostick resistivities respectively for the x-directed electric sensor in Line 2. Figures 11 and 12 show apparent resistivities and Bostick resistivities for the y-directed electric sensor. The apparent resistivity sections in Figures 10 and 12 are similar, but less so than were Figures 4 and 7 in Line 1, indicating an environment with more 2-D or 3-D effects. Both Bostick resistivity sections show a deep high conductivity zone that extends nearer the surface in the center of the section than at the edges. The location correlates with a previously mapped groundwater mound shown in Figure 13 (Geosystem Consultants, 1995), although this may not be the anomaly source. The mid-section anomaly is more pronounced and narrow in Figure 12 (y-directed electric receivers) than in Figure 10.

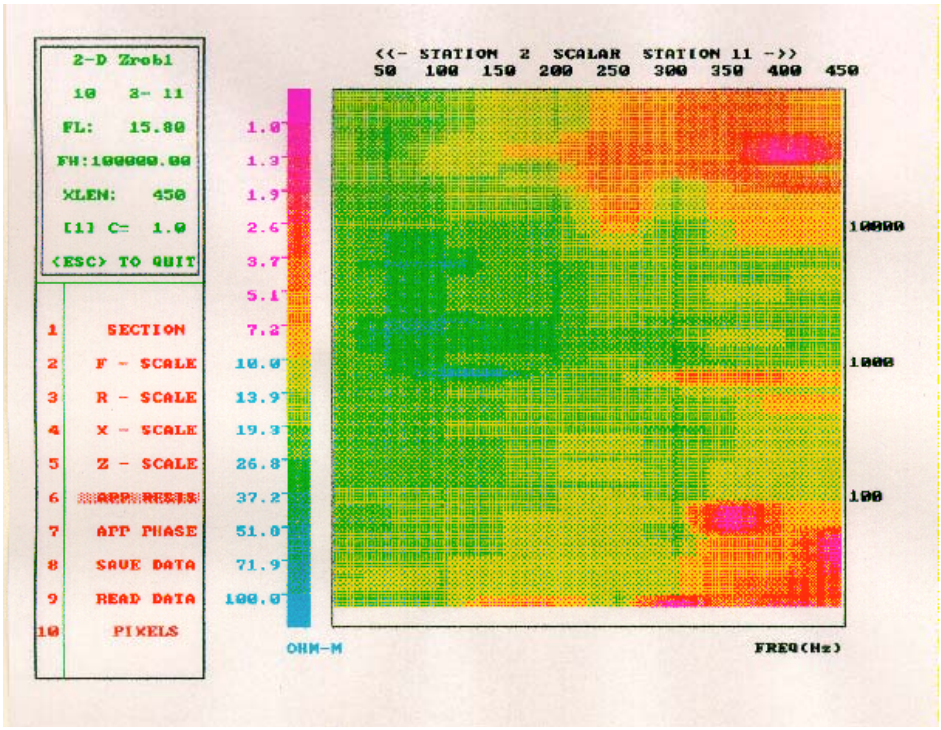

Figure 4. CSAMT apparent resistivity as a function of frequency, E_x/H_y, Line 1.

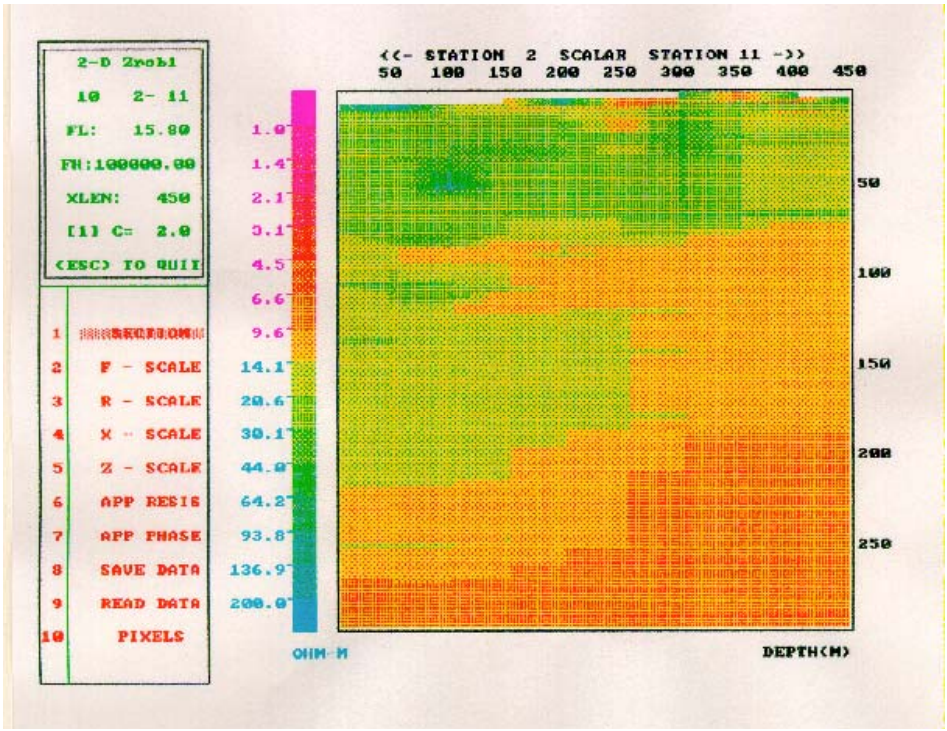

Figure 5. CSAMT Bostick resistivity as a function of depth, E_x/H_y, Line 1.

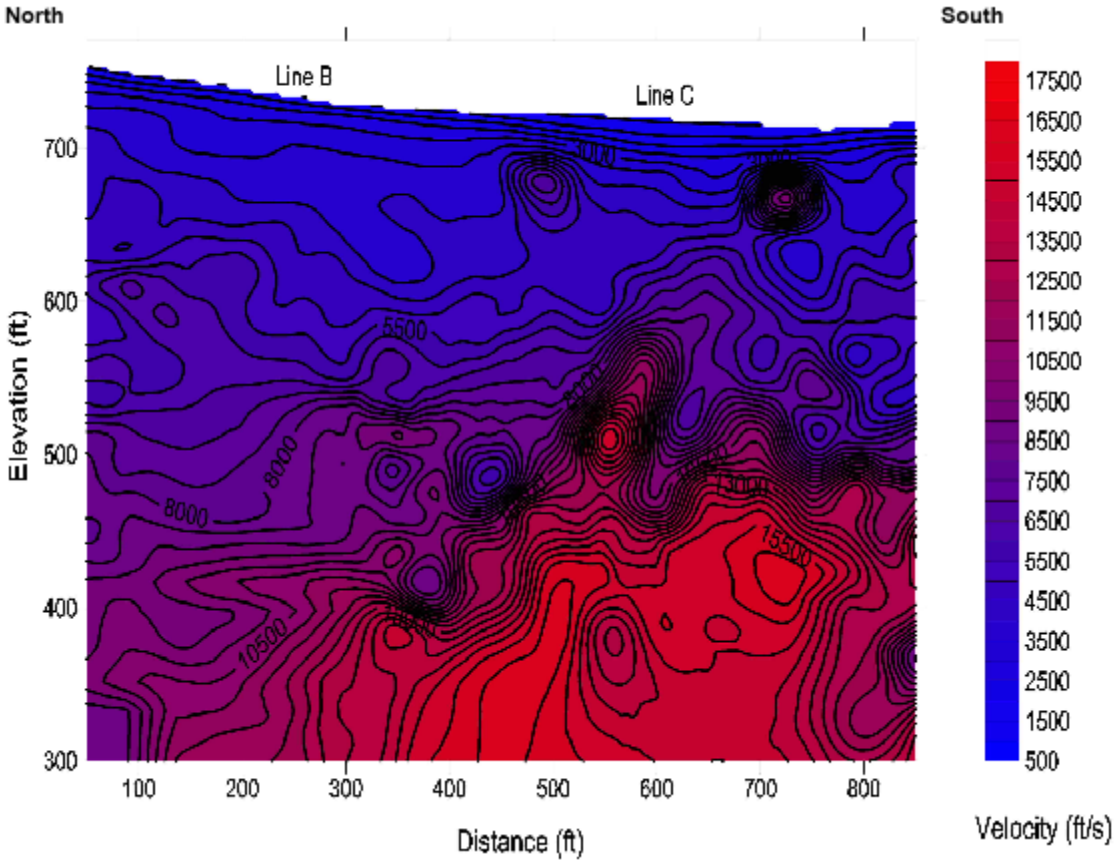

Figure 6. Tomographic 2-D seismic velocity inversion along seismic lines parallel to CSAMT Line 1 (From Doll et al., 2001). Referring to Figure 3, the north end of the line starts near TEM sounding site 6, and continues to the point marked C' at the southeast edge of Block 15.

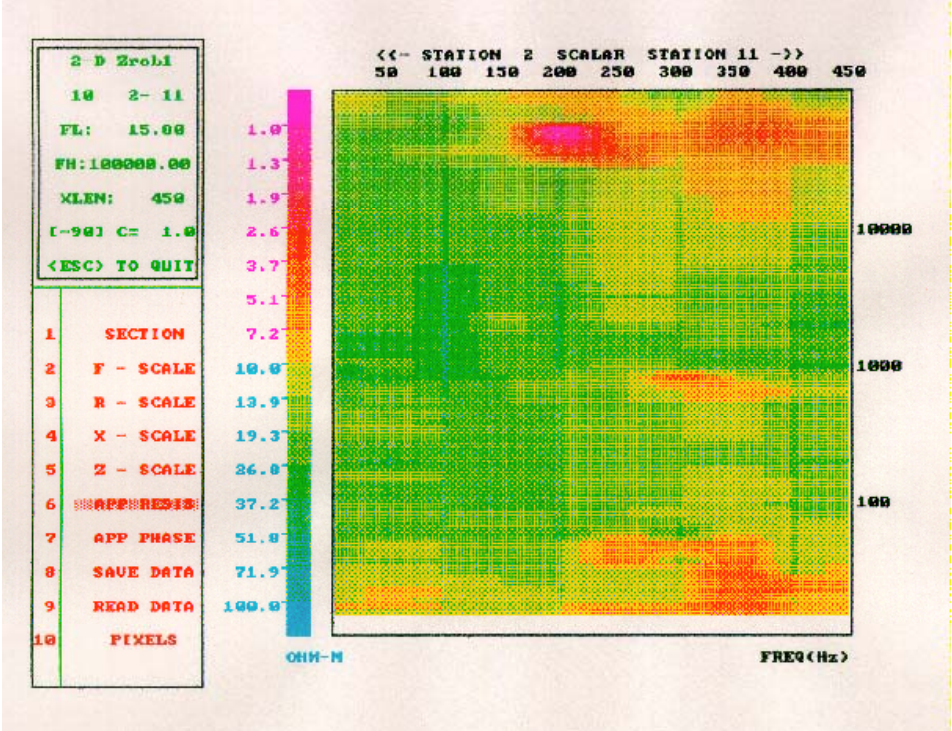

Figure 7. CSAMT apparent resistivity as a function of frequency, E_y/H_x, Line 1.

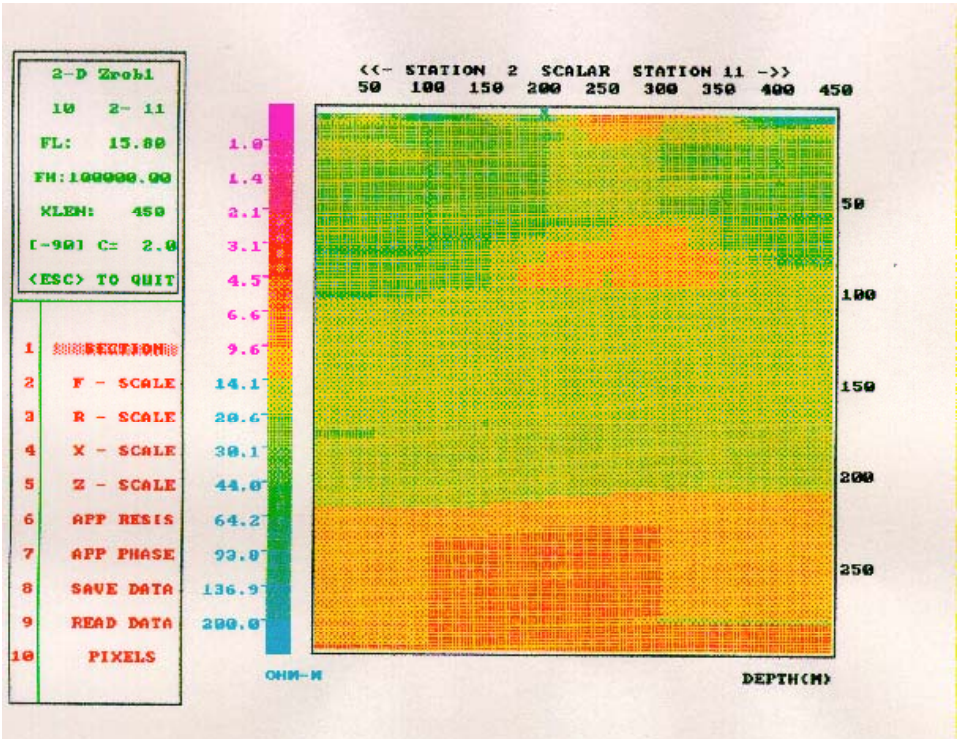

Figure 8. CSAMT Bostick resistivity as a function of depth, E_y/H_x, Line 1.

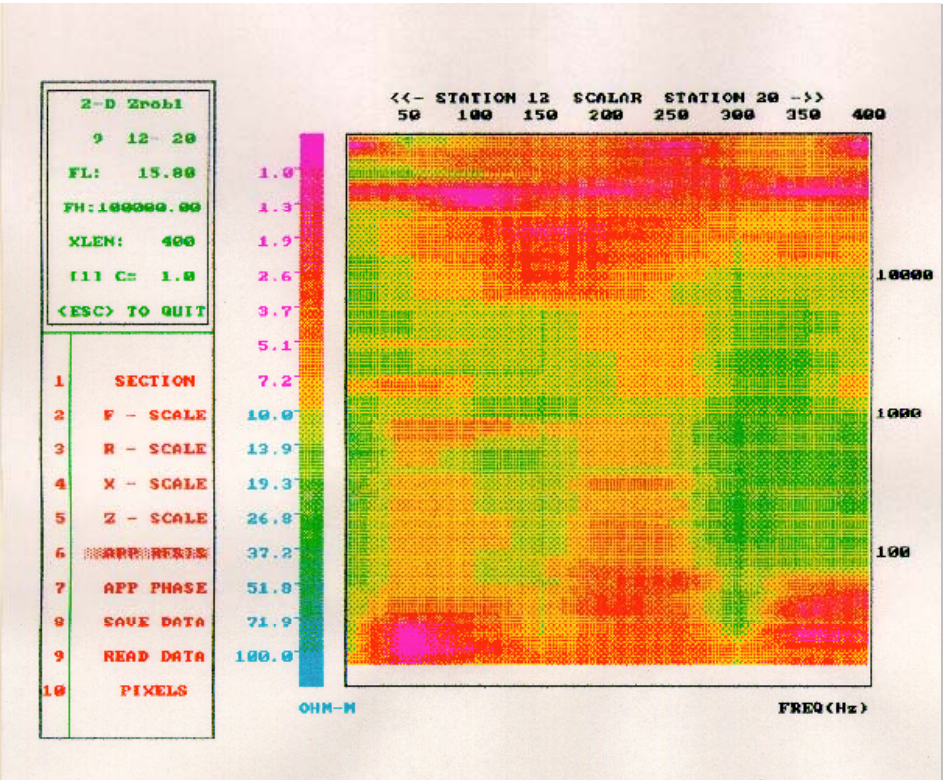

Figure 9. CSAMT apparent resistivity as a function of frequency, E_x/H_y, Line 2.

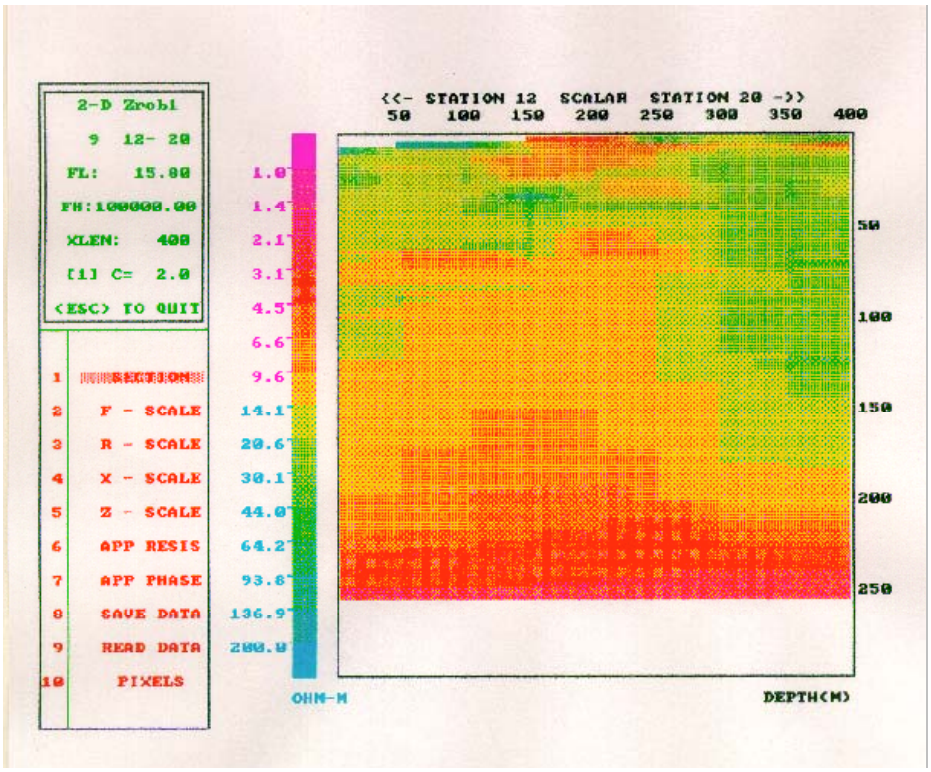

Figure 10. CSAMT Bostick resistivity as a function of depth, E_x/H_y, Line 2.

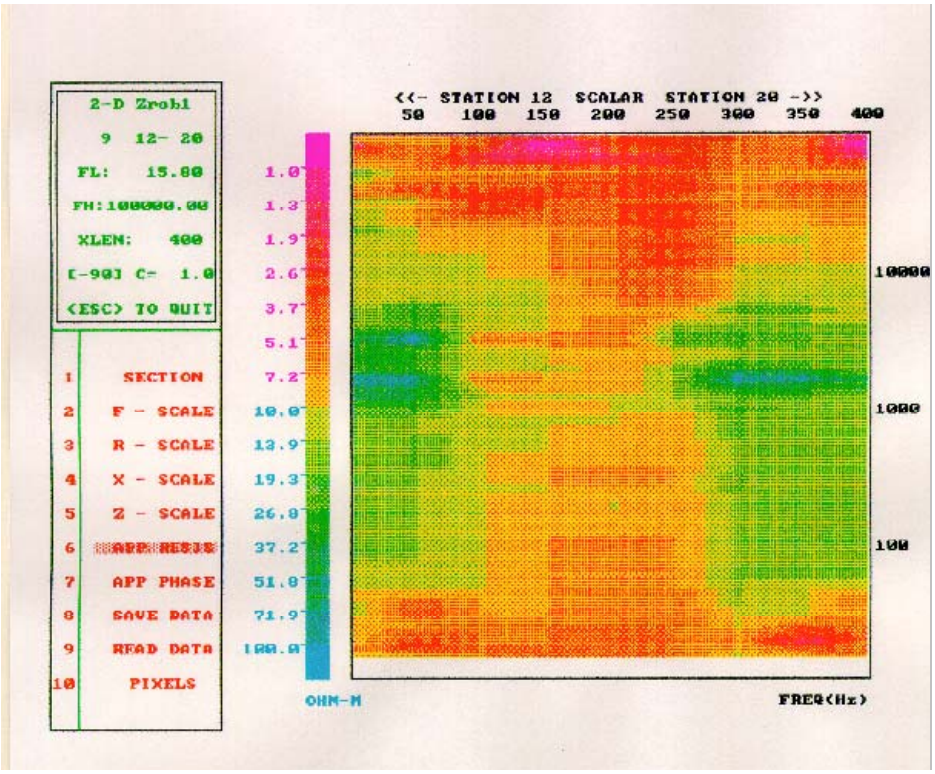

Figure 11. CSAMT apparent resistivity as a function of frequency, E_y/H_x, Line 2.

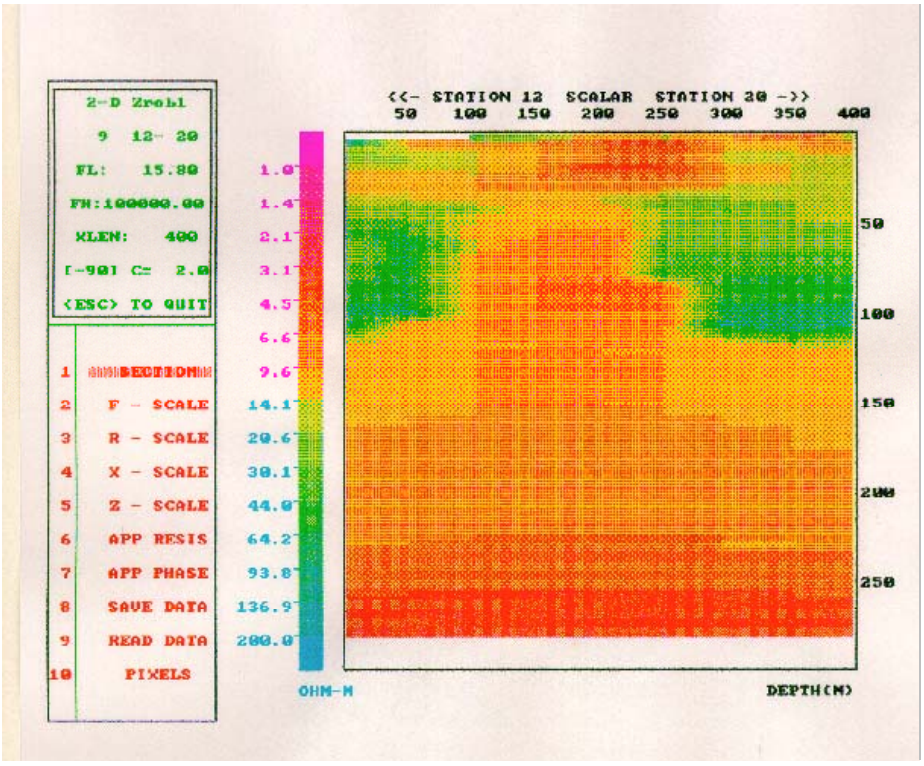

Figure 12. CSAMT Bostick resistivity as a function of depth, E_y/H_x, Line 2.

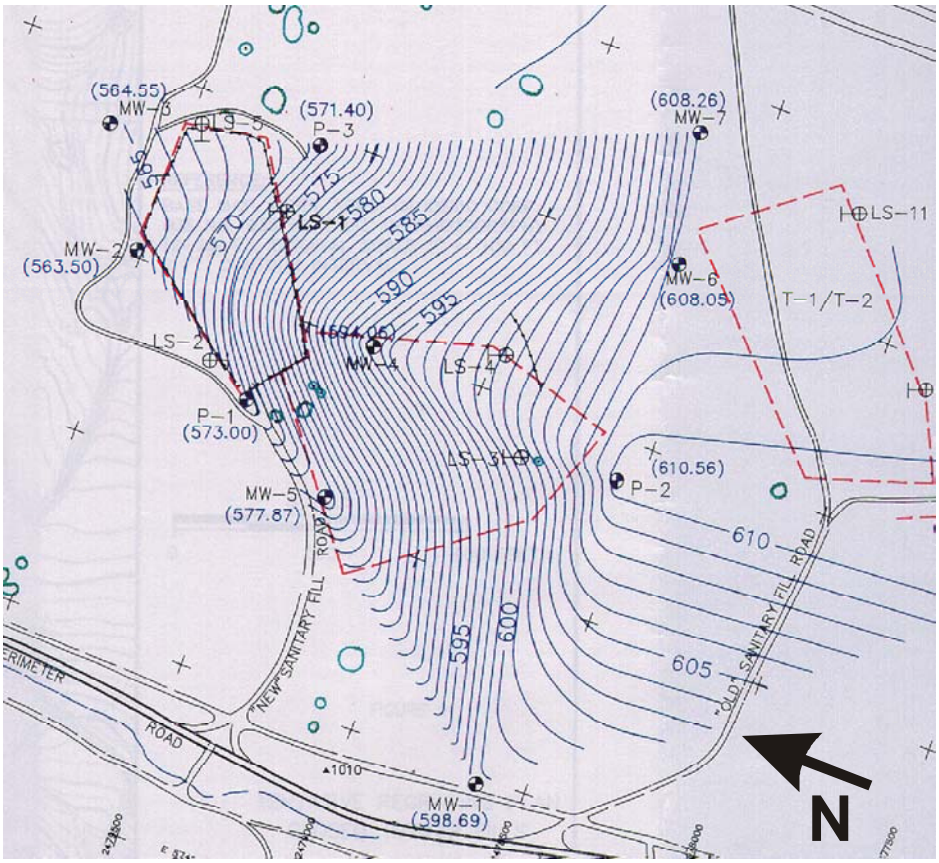

Figure 13. Ground water contours as measured on 21 October 1994. Units are in feet above mean sea level. Landfill units outlined in red. (Adapted from Figure 8, Geosystems, 1995.)

5.2 TEM Data

Transient EM data were of consistently high quality and needed little editing before entry into interpretation software. Noise levels were low for the first 19 time gates. Gate 20 was noisy at each of the 8 sounding sites, and was deleted from the data sets. At each site, three separate transient sounding curves were collected. In cases where the decay values for a particular time gate were different in all three sounding curves, the middle value was selected for inversion. However, in almost every case, the sounding curves showed nearly identical values at any given gate, another indication of an electrically low noise environment.

The TEM data were inverted using a horizontally layered earth model. The inversion algorithm (TEMIX XL by Stoyer et al., 1996) fit the data to a user chosen number of layers, adjusting the resistivity and thickness of each layer so that the difference between data computed from the layered earth model and the field data was minimized in a least squares sense. As can be seen in Appendix B, the model curves fit the data very well at all 8 sites. The site 5 TEM sounding, shown in Figure 14, is representative of 7 of the 8 sites. The data do not show any abrupt changes to indicate strong resistivity contrasts, suggesting a gradual decrease in electrical resistivity with depth, at least in the upper section. The computed apparent resistivity from a 7-layer model fits the measured apparent resistivity to within 2 percent.

The upper 60 meters has a resistivity of a few thousand ohm-m, indicative of unsaturated, if not completely dry, conditions. These high resistivities are at least in part a numerical artifact created by using a late time TEM apparent resistivity computation at early times. As shown by Spies and Frischknecht (1991) the late time approximation produces overly high resistivity estimates at early recording times. Furthermore, the first time gate is at 80 μs, a time corresponding to a current diffusion depth of about 60 m over a 30 ohm-m half space (a typical CSAMT resistivity). Thus, the TEM system is insensitive to the first few tens of meters below the surface.

However, beyond the 60 m depth, the resistivity decreases gradually to 100 ohm-m through the next 50 m, then at a depth of 110 m the resistivity decreases abruptly to 2 ohm-m in a relatively thin layer—15 m thick at this sounding location. The resistivity then abruptly increases to 100 ohm-m through a 50-m thick section, and then at 180 m depth decreases again to 10 ohm-m. The soundings in Appendix B show very similar patterns and depths at all locations except at sounding site 1. As no boreholes have been drilled to depths beyond 100 m, the source of the conductive layer is uncertain. A conductive layer is necessary for the model to fit the data, so in this sense it is not an artifact. It is possible that the transient method has set up currents in buried metallic debris in one of the waste burial areas, but in this case one would expect that the depth of the conductive layer would change as the transmitter loop was set up nearer or farther from the waste dump. As the depth to the top of the conductive zone is constant to within a few meters over 7 soundings, it is more likely the data reflects a widespread conductive zone at a depth of about 100 m.

The sounding at site 1 is different from the others in that it shows no thin high conductivity layer, and the resistivity of the near surface layer is an order of magnitude lower than at other sites. One side of the 100 m x 100 m transmitter loop at this site was laid 40-50 m from a grounded metal fence that surrounded the active waste disposal area. This may have been close enough to induce significant currents in the fencing and cause the currents to decay slowly, making the earth appear artificially more conductive by an order of magnitude and reducing the depth of investigation.

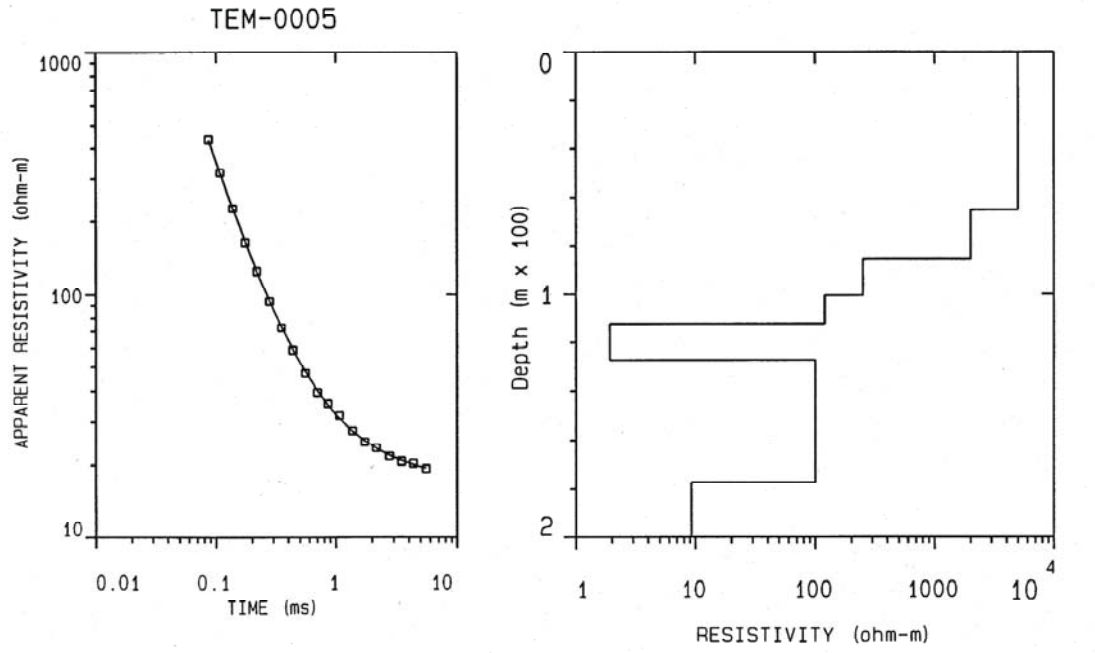

Figure 14. TEM sounding data and inversion results, site 5, Line 2, located at intersection of Lines 1 and 2.

6 DISCUSSION AND CONCLUSIONS

The electromagnetic sounding methods used in this study gathered information to depths greater than 200 meters, a depth well beyond any existing boreholes in the area, and also beyond the detection depth of previous geophysical surveys, with the exception of seismic refraction data. It is difficult to arrive at firm conclusions given this dearth of ground truth. I can however indicate the extent to which deep EM data are consistent with existing data, and I can suggest sources for the anomalies seen in the deep EM data.

For both EM sounding methods, data quality appears to be good. The error bars on the CSAMT data are mostly small, even for the lowest frequencies, and the repeatability of the TEM sounding data indicate a high signal-to-noise ratio. The topography at the landfill site was not extreme, and it is unlikely that topographic relief had a significant

effect on either the TEM or the CSAMT data. The lack of divergence of the ρ_x and ρ_y CSAMT curves indicate a 1-D earth approximation is valid.

The high frequency portion of the CSAMT data is in general agreement with DC resistivity profiles collected in a previous survey (Doll et al., 2000). The DC results show a thin conductive layer 2-3 meters thick overlying a resistive layer 10 or more meters thick. Both CSAMT lines show this character in their shallow sections. The TEM sites do not show the topmost thin conductive layer imaged by the DC resistivity data, and the shallow TEM resistivities are higher than both the CSAMT resistivities and the DC results. High TEM resistivities at early times (i.e., shallow depths) occur when the late time TEM apparent resistivity approximation is used to compute resistivities at early times (Spies and Frischknecht, 1991).

If the water table occurs at depths of less than 50 m as is indicated for 18 of 26 wells in Table 2 of the Geosystems report (1995), then it is not being clearly detected with either TEM, CSAMT, or seismic refraction. Doll et al. (2000) note that the seismic data indicate a gradational increase in velocity with depth rather than an abrupt change. This would make a seismic determination of the water table depth difficult. Near-surface heterogeneity or thin high velocity layers above the water table could also prevent its detection with seismic refraction. TEM and CSAMT data also show gradational changes. None of the 8 TEM sounding curves (Appendix B) show abrupt changes indicative of thick layers of high electrical contrast. The inversion models for each TEM sounding show 3 or more layers in the upper 100 m with each deeper layer becoming increasingly conductive. The water table as reported by Geosystems is not obviously connected with any of the resistivity interfaces. The first resistivity interface occurs at a depth of 60-80 m, 10 or more meters deeper than the range of the majority of groundwater depths recorded in Table 2 of the Geosystems report (1995). The TEM models show a resistivity drop from a high resistivity layer of several thousand ohm-m, the dry upper section of the earth, to a moister layer having a resistivity of about 2000 ohm-m. Such a high resistivity indicates either unsaturated conditions or, if saturated, then fresh water.

The inability of the two methods to give clear evidence of the water table at depths indicated by boreholes may simply mean there is insufficient electrical contrast for unambiguous detection. However, if the water table is perched, structurally truncated, or otherwise localized, then the electromagnetic data may be telling more about the water table than is initially apparent.

Of particular interest in the TEM data is a thin, very conductive layer that occurs at a depth of about 100 m. Its inverted thickness is only 10-20 m, but it has the effect of causing the apparent resistivity curve to flatten out slightly, and models without this layer produce poor fits to the data. Its depth is below that of the wells drilled in the area, so there is no immediate way to verify the existence of the layer. The resistivity of the layer is about 2 ohm-m. From Archie's relation $\rho_{formation} = \rho_{pore\_water} / \phi^2$ where ϕ is porosity, a 2 ohm-m formation resistivity implies a pore water resistivity of less than 0.1 to 0.5 ohm-m. This translates to a sodium chloride concentration of 20000 mg/l or more (Keys,

1989, Figure 19 as modified from Alger, 1966), about the equivalent concentration of seawater, and seemingly too high and too deep to be related to landfill contamination. Alternative explanations for such high conductivities are sulfide mineralization, or the presence of a graphitic zone related to tectonic stresses (Korya and Hjelt, 1998), but these explanations seem unlikely in this geologic setting. I judge the saline water explanation to be the most likely, even though the layer is probably not deep enough to be part of the Pancho Rico, a formation of marine origin. The thin conductive layer does not appear on the CSAMT data, although thicker conductive zones show up at depths of between 70 and 110 m on both lines. This apparent lack of correspondence might derive from the smoothness of the Bostick inversion method. Under Bostick inversion, thin conductive layers would appear thicker and less conductive than in a layered earth inversion.

A feature common to both the TEM and CSAMT data is a basal conductive layer of about 10 ohm-m at 180-200 m depth. This resistivity translates to about 1 ohm-m, representative of brackish pore water, and might represent the top of the Pancho Rico formation.

The above conclusions are based on 1-D inversions of CSAMT and TEM data. Some of the differences seen in comparing the E_x/H_y CSAMT resistivity sections to the E_y/H_x resistivity sections might be resolved using 2-D inversion. In particular, the question of the shallowing of the conductive layer at the south end of Line 1 might be resolved with 2-D modeling. TEM soundings were spaced at 100 m intervals with only 4 soundings along each line. These data would not benefit greatly from 2-D or 3-D modeling or inversion.

7 RECOMMENDATIONS

At least two results stand out as worthy of further attention. The deep conductive zone that rises sharply near CSAMT station 6 (x = 250 m) on Line 1 also shows up on seismic refraction data (Doll et al., 2000). The top of the conductive zone appears deeper than the top of the seismic high velocity zone, and the break appears further to the north than in the seismic data, but the lines are 100 m apart and the strike of the controlling structure is not known. If a fault caused the apparent offset in the geophysical properties, this could have important implications with respect to possible contamination migration routes. Additional borehole and/or seismic reflection data could help resolve this question.

The thin, highly conductive layer that appears in the TEM sounding data at a depth of about 100 m appears to be a widespread feature. It is unlikely that the high conductivity is caused by contamination from the overlying landfill. A deep borehole could resolve this issue.

8 ACKNOWLEDGMENTS

Barry Kinsall, ORNL, assisted in data collection and collected GPS data at each of the receiver and transmitter sites. John Morrow, Remedial Program Manager for the Camp Roberts Installation Restoration Program, assisted in data collection and provided logistical support. Jeff Johnston of Geometrics provided instruction in the use of the STRATAGEM EH-4 CSAMT system. Oak Ridge National Laboratory is managed by UT-Battelle, LLC for the U. S. Department of Energy under contract DE-AC05-00OR22725. This manuscript has been authored by a contractor of the U. S. Government. Accordingly, the U. S. Government retains a nonexclusive, royalty-free license to publish or reproduce the published form of this contribution, or allow others to do so, for U. S. Government purposes.

9 REFERENCES

Alger, R.P., 1966. Interpretation of electric logs in freshwater wells in unconsolidated formations: Proceedings of the SPWLA 7th Annual Symposium, Tulsa, pp. CC1-CC25.

Bostick, F.X., 1977. A simple almost exact method of MT analysis: Workshop on Electrical Methods in Geothermal Exploration, U.S. Geological Survey Contract No. 14080001-8-359.

Doll, W.E., Gamey, T.J., Nyquist, J.E., Mandell, W., Groom, D., and Rohdewald, S., 2001. Evaluation of new geophysical tools for investigation of a landfill, Camp Roberts, California: Expanded abstract in SAGEEP 2001 Proceedings.

Doll, W.E., Gamey, T.J., and Nyquist, J.E., 2000. Geophysical investigation of the Camp Roberts Sanitary Landfill, San Luis Obispo County, California: Report for U.S. Army Environmental Center, 38 pp.

Geometrics, 2000. STRATAGEM operation manual, Geometrics, Inc., 38 pp.

Geonics, 1999. Protem 57 D operating manual for 20/30 gate model, Geonics, Ltd., 55 pp.

Geosystem Consultants, 1995. Additional site characterization, fourth quarter 1994 detection monitoring, and annual detection monitoring summary: Report of Project No. 92-488, Geosystem Consulatants, Inc.

Keller, G., 1988. Chapter 2, Rock and mineral properties *in* Electromagnetic methods in applied geophysics, volume 1 (M. Nabighian, Ed.), Society of Exploration Geophysicists, 513 pp.

Keys, W.S., 1989. Borehole geophysics applied to ground-water investigations: National Ground Water Association, 313 pp.

Korja T. and Hjelt, S.E., 1998. The Fennoscandian Shield: a treasure box for deep electromagnetic studies *in* Deep Electromagnetic Exploration (K.K. Roy, S.K. Verma, and K. Mallick, Eds.), 31-73.

Spies, B.R. and Frischknecht, F.C., 1991. Chapter 5, Electromagnetic sounding *in* Electromagnetic methods in applied geophysics, volume 2 (M. Nabighian, Ed.), Society of Exploration Geophysicists, 972 pp.

Stoyer, C.H., Zerilli, A., Wilson, G., and Butler, M.S., 1996. TEMIX XL v4 Transient electromagnetic data interpretation software User's Manual, Interpex Ltd., 329 pp.

Zonge, K.L. and Hughes, L.J., 1991. Chapter 9, Controlled source audio-frequency magnetotellurics *in* Electromagnetic methods in applied geophysics, volume 2 (M. Nabighian, Ed.), Society of Exploration Geophysicists, 972 pp.

10 APPENDIX I—CSAMT soundings

The sounding results for each CSAMT site are shown in Appendix I. Line 1 consists of stations 2-11, beginning at the north end of the line. Stations 12-20 make up Line 2 with station 12 at the east end of the line. Data shown are apparent resistivity, phase, coherence, and Bostick resistivity.

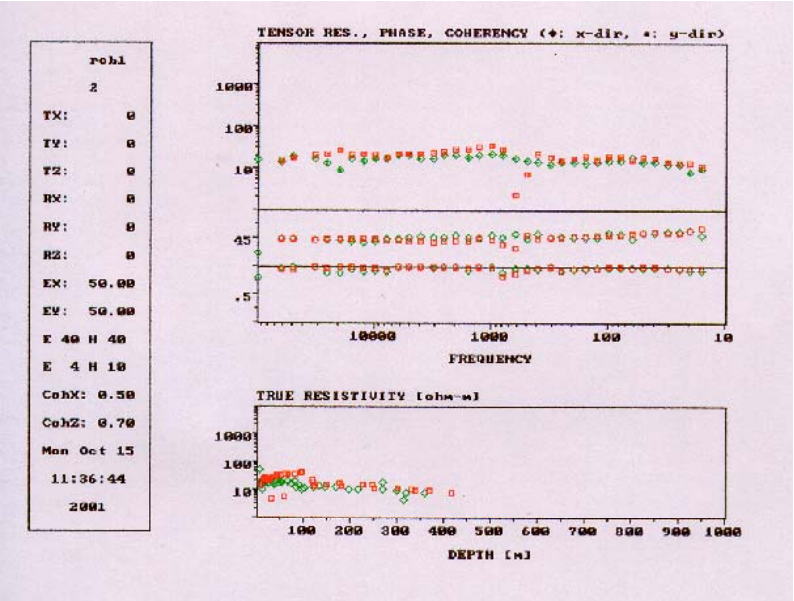

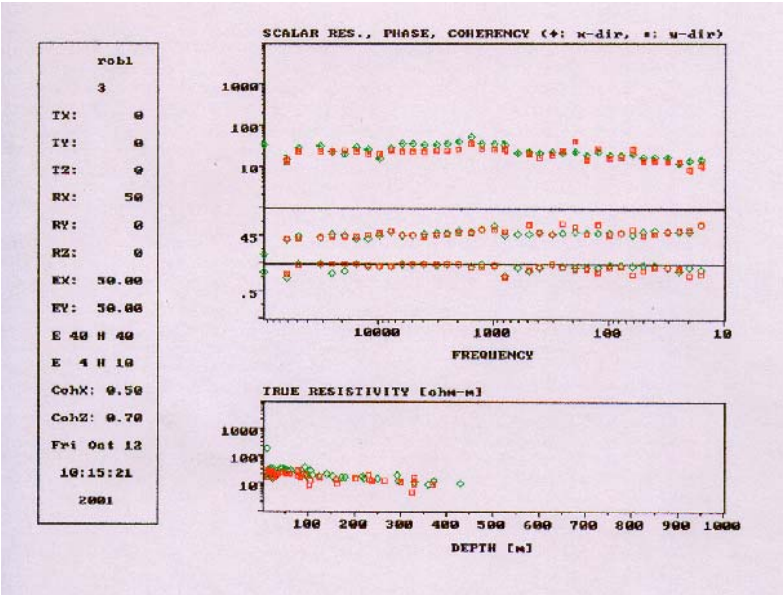

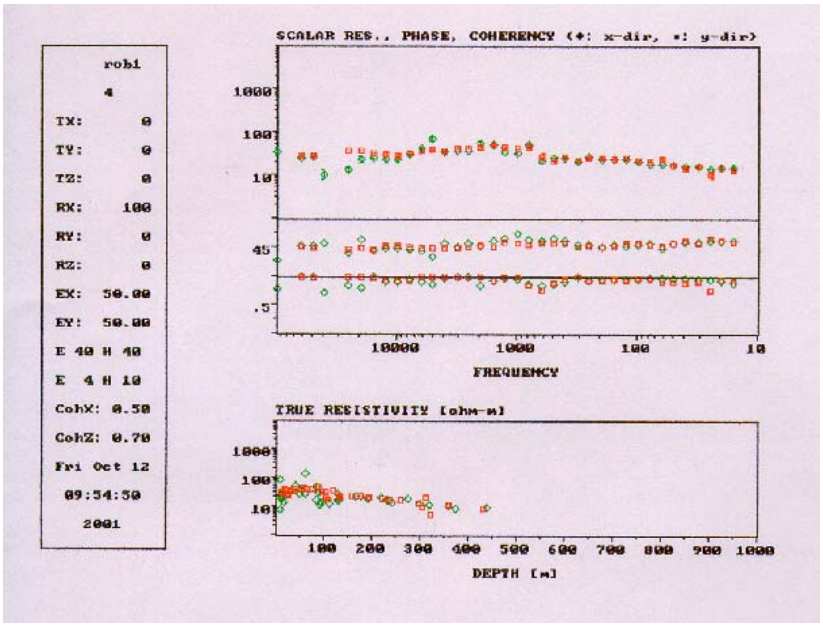
rob1
4
TX: 0
TY: 0
TZ: 0
RX: 100
RY: 0
RZ: 0
EX: 50.00
EY: 50.00
E 40 H 40
E 4 H 10
CohX: 0.50
CohZ: 0.70
Fri Oct 12
09:54:50
2001
SCALAR RES., PHASE, COHERENCY (+: x-dir, •: y-dir)
1000
100
10
45
.5
10000
1000
100
10
FREQUENCY
TRUE RESISTIVITY [ohm-m]
1000
100
10
100 200 300 400 500 600 700 800 900 1000
DEPTH [m]

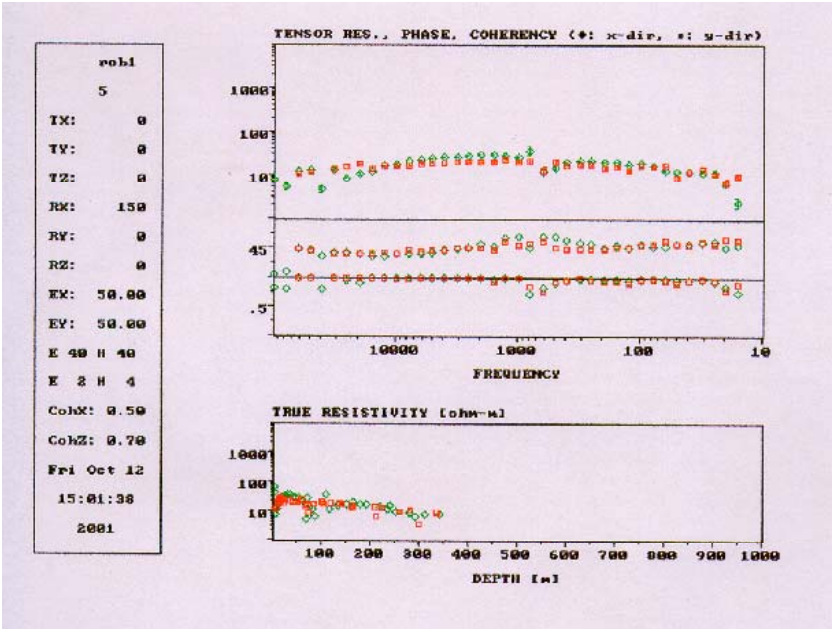
rob1
5
TX: 0
TY: 0
TZ: 0
RX: 150
RY: 0
RZ: 0
EX: 50.00
EY: 50.00
E 40 H 40
E 2 H 4
CohX: 0.50
CohZ: 0.70
Fri Oct 12
15:01:38
2001
TENSOR RES., PHASE, COHERENCY (+: x-dir, •: y-dir)
1000
100
10
45
.5
10000
1000
100
10
FREQUENCY
TRUE RESISTIVITY [ohm-m]
1000
100
10
100 200 300 400 500 600 700 800 900 1000
DEPTH [m]

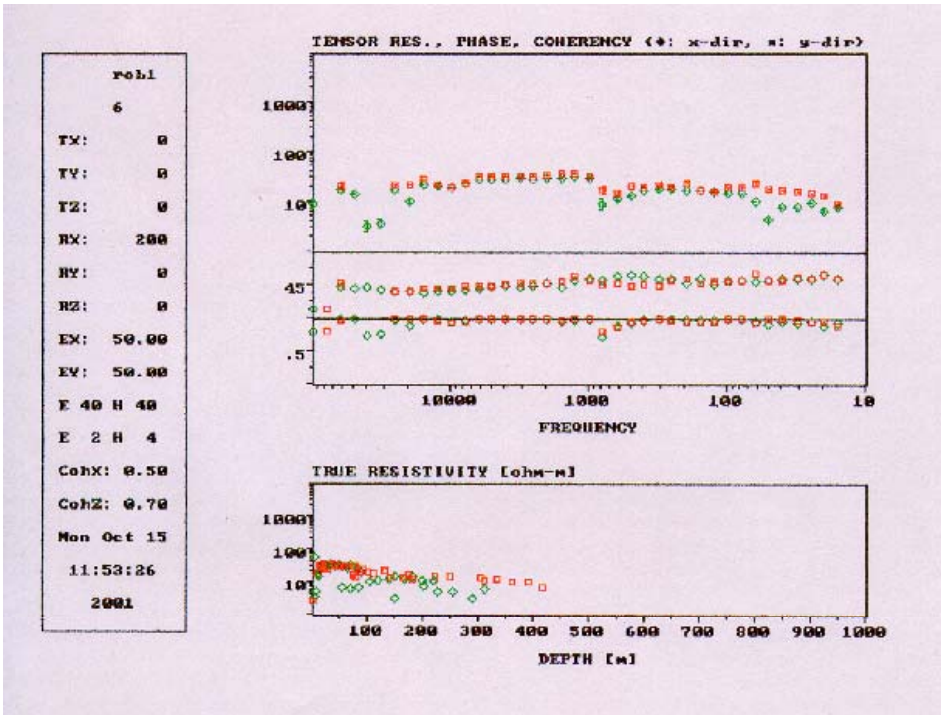
rob1
6
TX: 0
TY: 0
TZ: 0
RX: 200
RY: 0
RZ: 0
EX: 50.00
EY: 50.00
E 40 H 40
E 2 H 4
CohX: 0.50
CohZ: 0.70
Mon Oct 15
11:53:26
2001
TENSOR RES., PHASE, COHERENCY (♦: x-dir, ×: y-dir)
1000
100
10
45
.5
10000
1000
100
10
FREQUENCY
TRUE RESISTIVITY [ohm-m]
1000
100
10
100 200 300 400 500 600 700 800 900 1000
DEPTH [m]

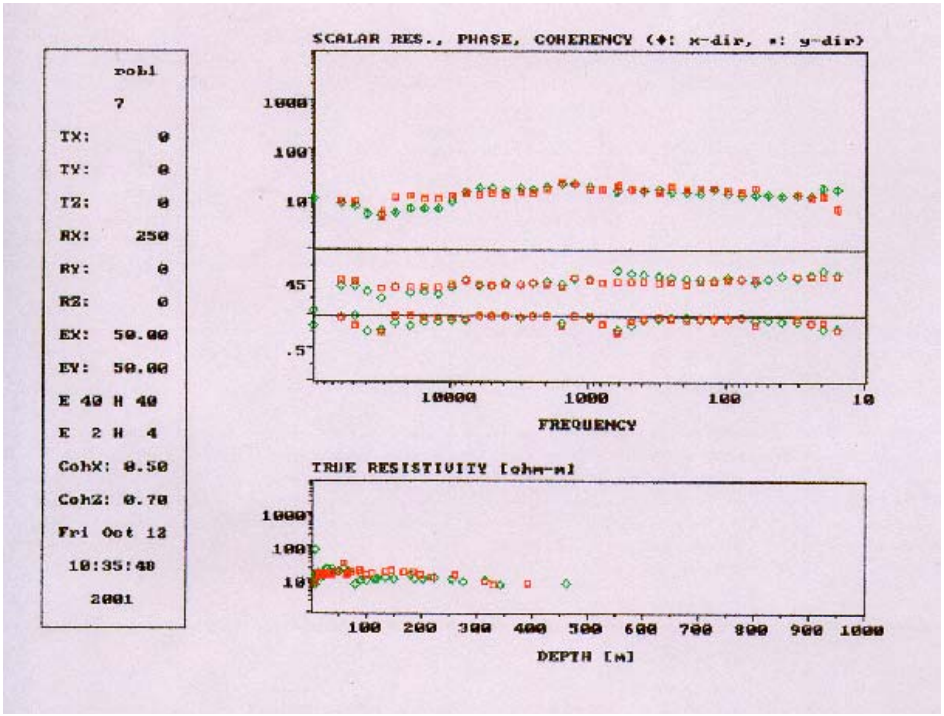
rob1
7
TX: 0
TY: 0
TZ: 0
RX: 250
RY: 0
RZ: 0
EX: 50.00
EY: 50.00
E 40 H 40
E 2 H 4
CohX: 0.50
CohZ: 0.70
Fri Oct 12
10:35:40
2001
SCALAR RES., PHASE, COHERENCY (♦: x-dir, ×: y-dir)
1000
100
10
45
.5
10000
1000
100
10
FREQUENCY
TRUE RESISTIVITY [ohm-m]
1000
100
10
100 200 300 400 500 600 700 800 900 1000
DEPTH [m]

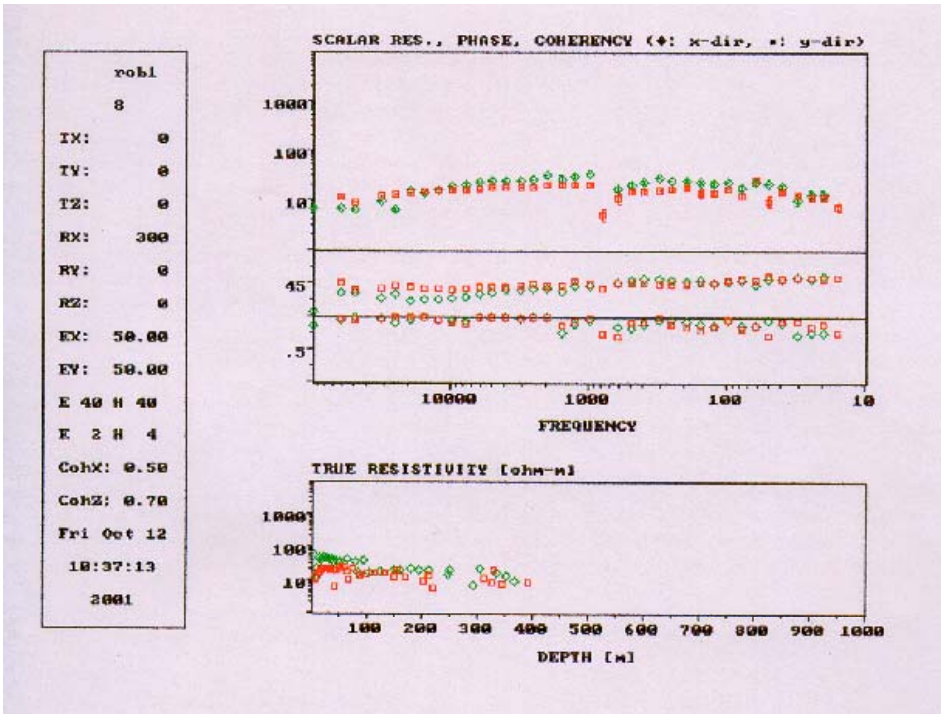
robl
8
TX: 0
TY: 0
TZ: 0
RX: 300
RY: 0
RZ: 0
EX: 50.00
EY: 50.00
E 40 H 40
E 2 H 4
CohX: 0.50
CohZ: 0.70
Fri Oct 12
10:37:13
2001
SCALAR RES., PHASE, COHERENCY (+: x-dir, *: y-dir)
1000
100
10
45
.5
10000
1000
100
10
FREQUENCY
TRUE RESISTIVITY [ohm-m]
1000
100
10
100 200 300 400 500 600 700 800 900 1000
DEPTH [m]

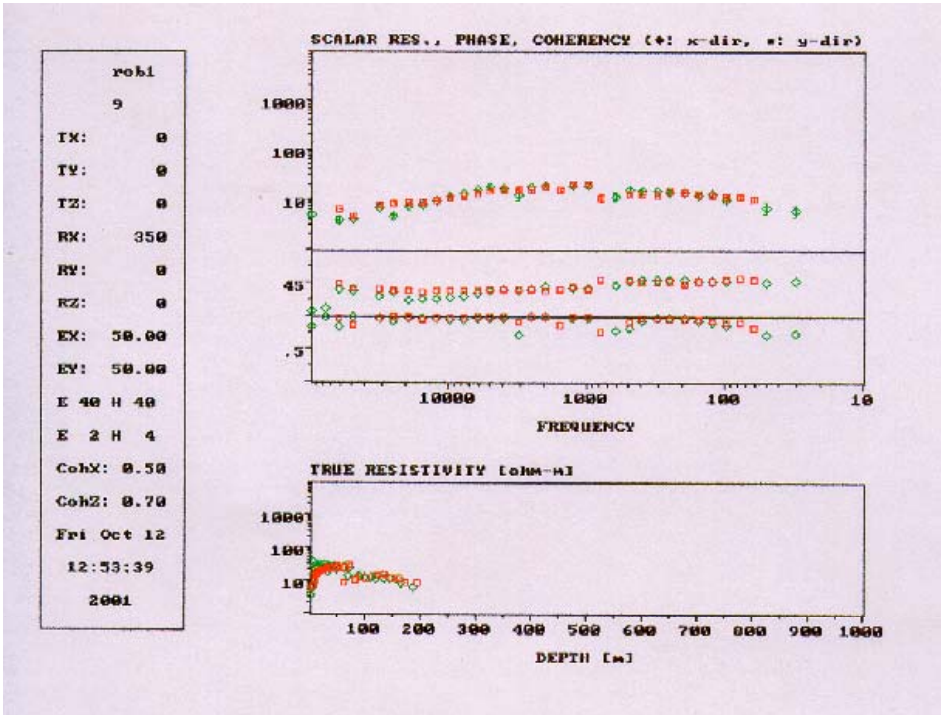
robl
9
TX: 0
TY: 0
TZ: 0
RX: 350
RY: 0
RZ: 0
EX: 50.00
EY: 50.00
E 40 H 40
E 2 H 4
CohX: 0.50
CohZ: 0.70
Fri Oct 12
12:53:39
2001
SCALAR RES., PHASE, COHERENCY (+: x-dir, *: y-dir)
1000
100
10
45
.5
10000
1000
100
10
FREQUENCY
TRUE RESISTIVITY [ohm-m]
1000
100
10
100 200 300 400 500 600 700 800 900 1000
DEPTH [m]

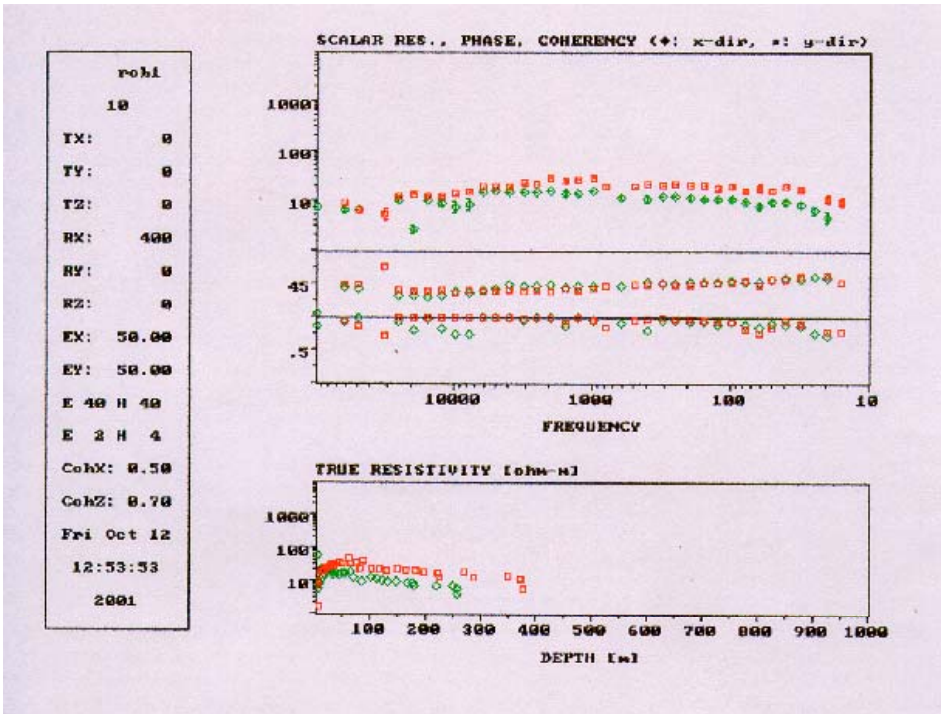
rohi
10
TX: 0
TY: 0
TZ: 0
RX: 400
RY: 0
RZ: 0
EX: 50.00
EY: 50.00
E 40 H 40
E 2 H 4
CohX: 0.50
CohZ: 0.70
Fri Oct 12
12:53:53
2001
SCALAR RES., PHASE, COHERENCY (+: x-dir, *: y-dir)
1000
100
10
45
.5
10000
1000
100
10
FREQUENCY
TRUE RESISTIVITY [ohm-m]
1000
100
10
100 200 300 400 500 600 700 800 900 1000
DEPTH [m]

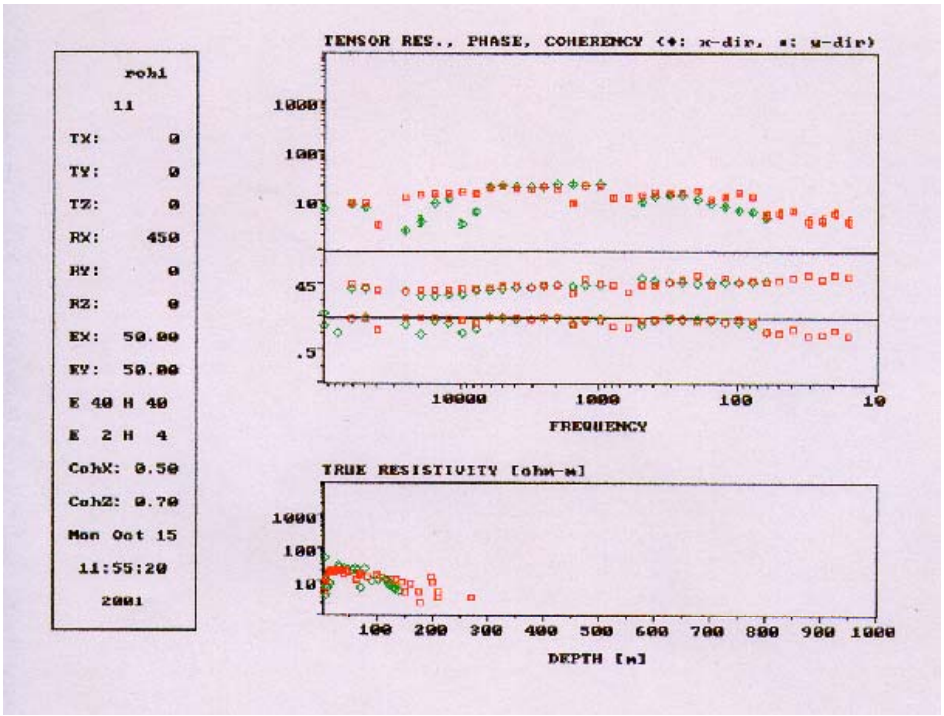
rohi
11
TX: 0
TY: 0
TZ: 0
RX: 450
RY: 0
RZ: 0
EX: 50.00
EY: 50.00
E 40 H 40
E 2 H 4
CohX: 0.50
CohZ: 0.70
Mon Oct 15
11:55:20
2001
TENSOR RES., PHASE, COHERENCY (+: x-dir, *: y-dir)
1000
100
10
45
.5
10000
1000
100
10
FREQUENCY
TRUE RESISTIVITY [ohm-m]
1000
100
10
100 200 300 400 500 600 700 800 900 1000
DEPTH [m]

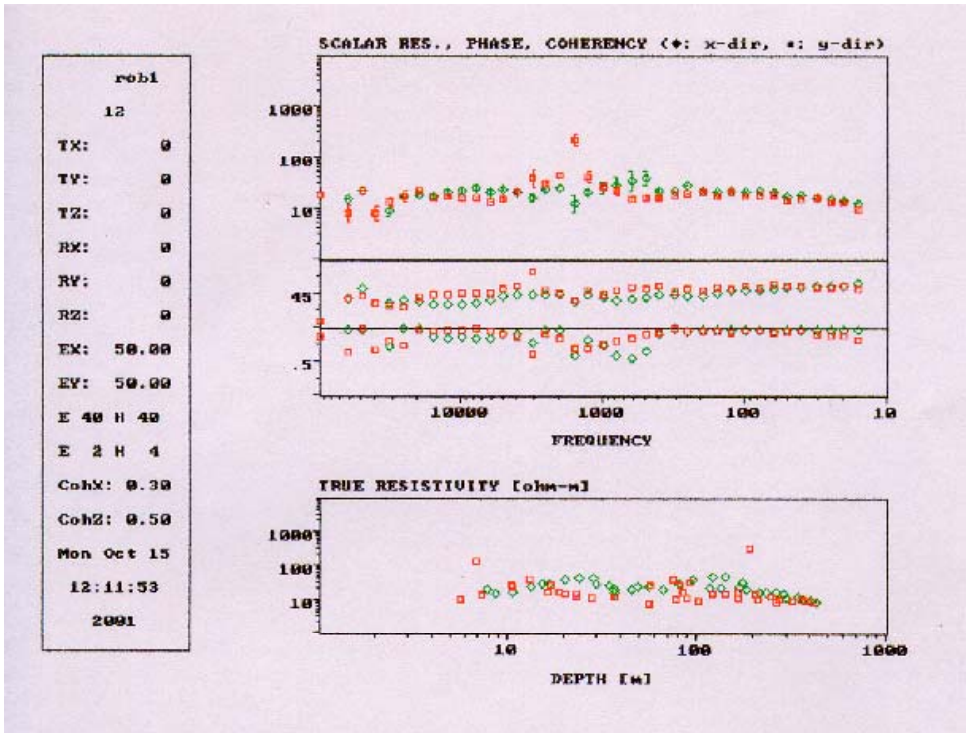
rob1
12
TX: 0
TY: 0
TZ: 0
RX: 0
RY: 0
RZ: 0
EX: 50.00
EY: 50.00
E 40 H 40
E 2 H 4
CohX: 0.30
CohZ: 0.50
Mon Oct 15
12:11:53
2001
SCALAR RES., PHASE, COHERENCY (+: x-dir, *: y-dir)
1000
100
10
45
.5
10000
1000
100
10
FREQUENCY
TRUE RESISTIVITY [ohm-m]
1000
100
10
10
100
1000
DEPTH [m]

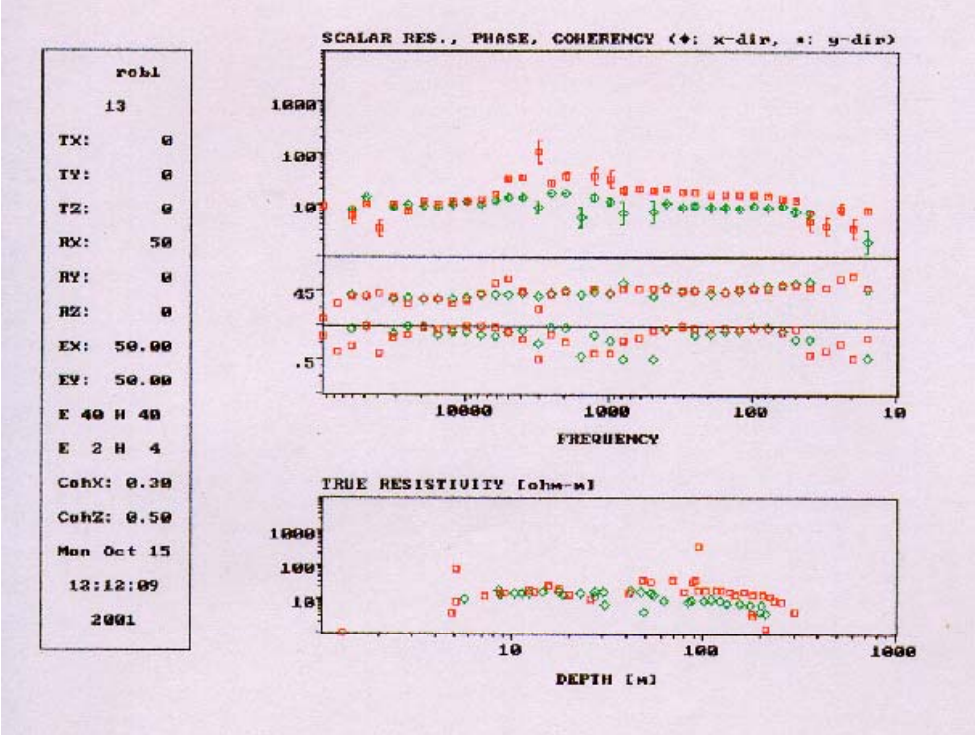
rob1
13
TX: 0
TY: 0
TZ: 0
RX: 50
RY: 0
RZ: 0
EX: 50.00
EY: 50.00
E 40 H 40
E 2 H 4
CohX: 0.30
CohZ: 0.50
Mon Oct 15
12:12:09
2001
SCALAR RES., PHASE, COHERENCY (+: x-dir, *: y-dir)
1000
100
10
45
.5
10000
1000
100
10
FREQUENCY
TRUE RESISTIVITY [ohm-m]
1000
100
10
10
100
1000
DEPTH [m]

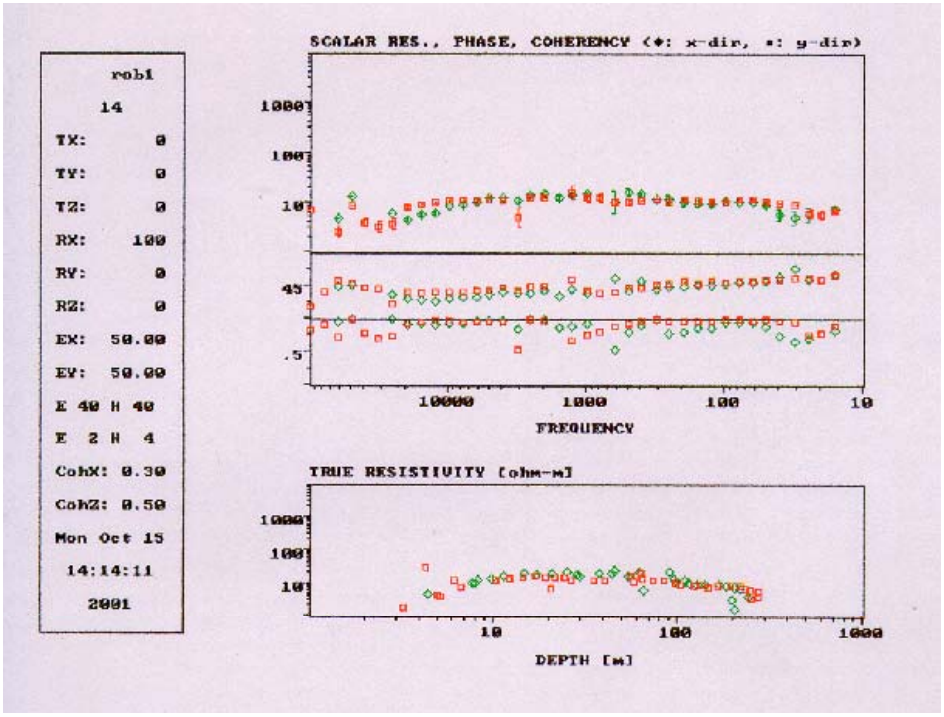
rob1
14
TX: 0
TY: 0
TZ: 0
RX: 100
RY: 0
RZ: 0
EX: 50.00
EY: 50.00
E 40 H 40
E 2 H 4
CohX: 0.30
CohZ: 0.50
Mon Oct 15
14:14:11
2001
SCALAR RES., PHASE, COHERENCY (+: x-dir, *: y-dir)
1000
100
10
45
.5
10000
1000
100
10
FREQUENCY
TRUE RESISTIVITY [ohm-m]
1000
100
10
10
100
1000
DEPTH [m]

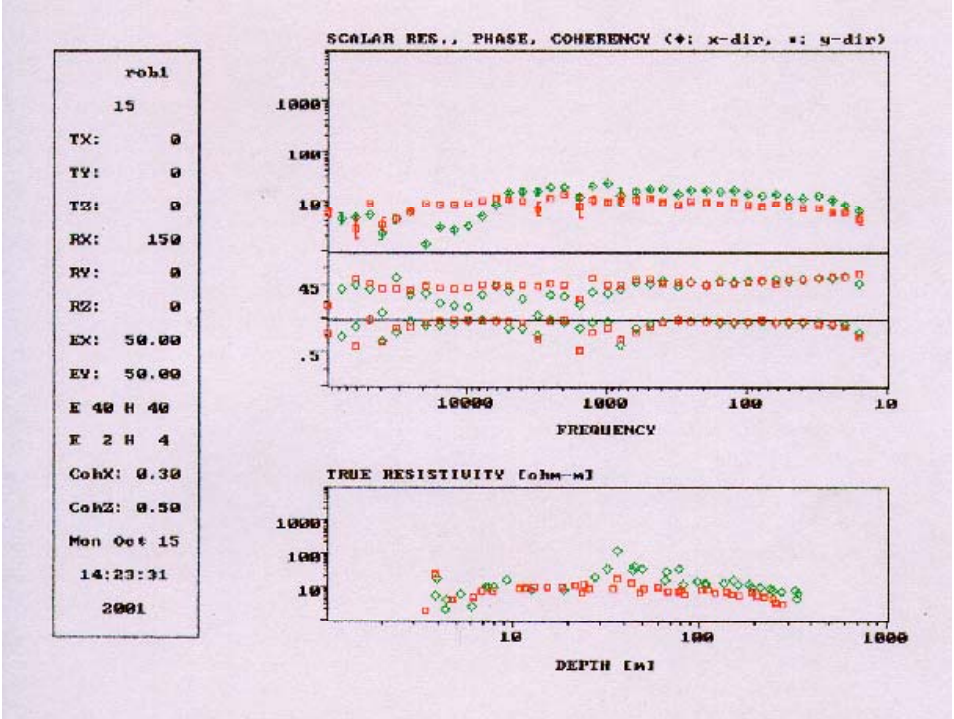
rob1
15
TX: 0
TY: 0
TZ: 0
RX: 150
RY: 0
RZ: 0
EX: 50.00
EY: 50.00
E 40 H 40
E 2 H 4
CohX: 0.30
CohZ: 0.50
Mon Oct 15
14:23:31
2001
SCALAR RES., PHASE, COHERENCY (+: x-dir, *: y-dir)
1000
100
10
45
.5
10000
1000
100
10
FREQUENCY
TRUE RESISTIVITY [ohm-m]
1000
100
10
10
100
1000
DEPTH [m]

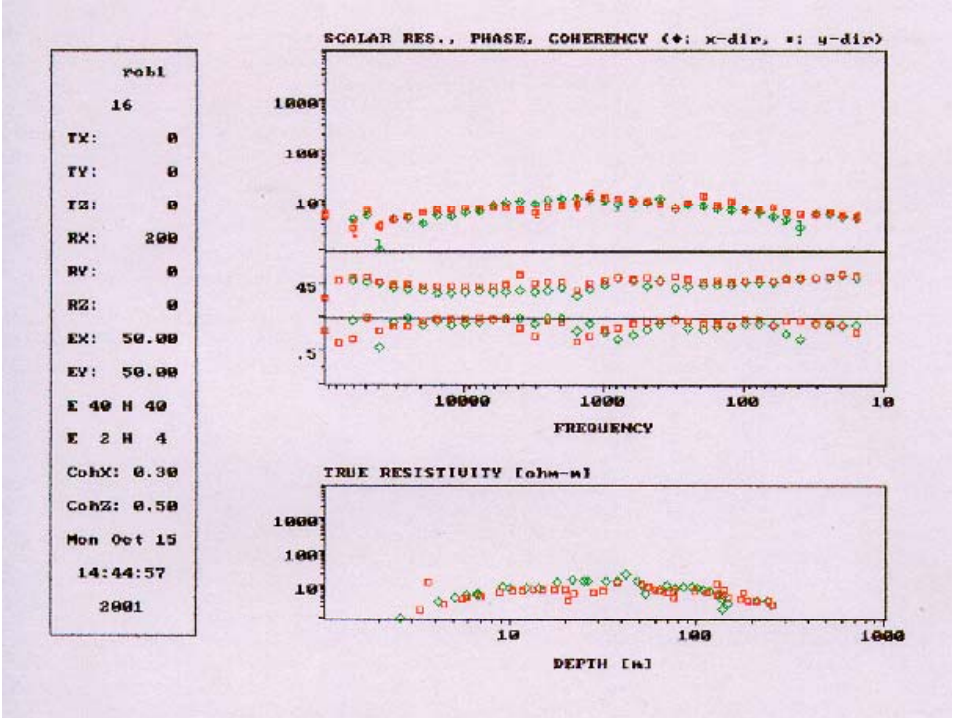
rob1
16
TX: 0
TY: 0
TZ: 0
RX: 200
RY: 0
RZ: 0
EX: 50.00
EY: 50.00
E 40 H 40
E 2 H 4
CohX: 0.30
CohZ: 0.50
Mon Oct 15
14:44:57
2001
SCALAR RES., PHASE, COHERENCY (+: x-dir, *: y-dir)
1000
100
10
45
.5
10000
1000
100
10
FREQUENCY
TRUE RESISTIVITY [ohm-m]
1000
100
10
10
100
1000
DEPTH [m]

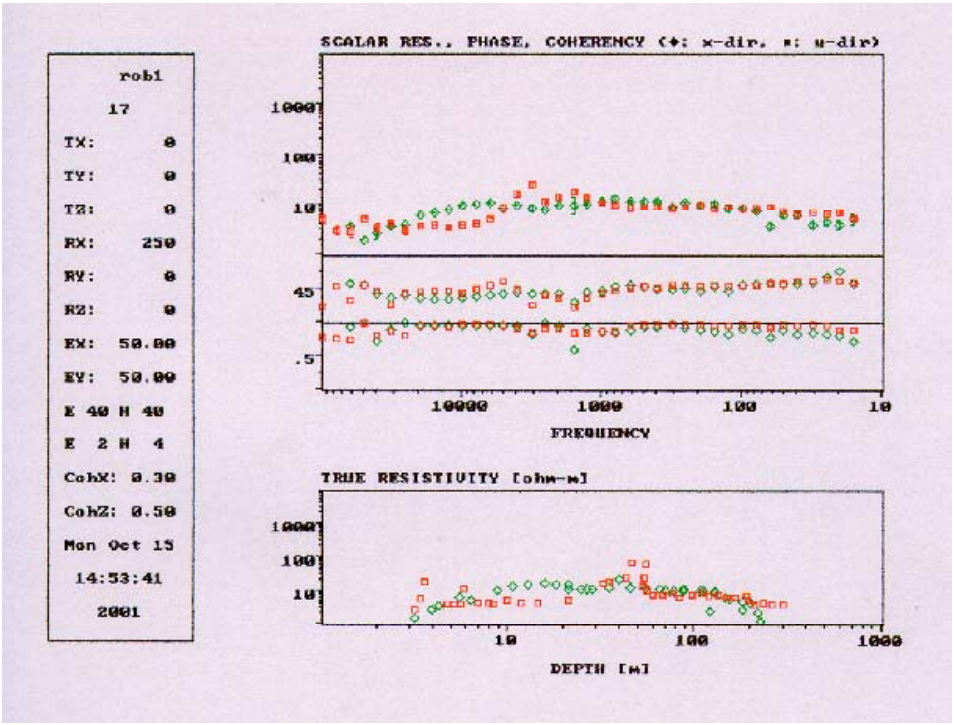
rob1
17
TX: 0
TY: 0
TZ: 0
RX: 250
RY: 0
RZ: 0
EX: 50.00
EY: 50.00
E 40 H 40
E 2 H 4
CohX: 0.30
CohZ: 0.50
Mon Oct 15
14:53:41
2001
SCALAR RES., PHASE, COHERENCY (+: x-dir, *: y-dir)
1000
100
10
45
.5
10000
1000
100
10
FREQUENCY
TRUE RESISTIVITY [ohm-m]
1000
100
10
10
100
1000
DEPTH [m]

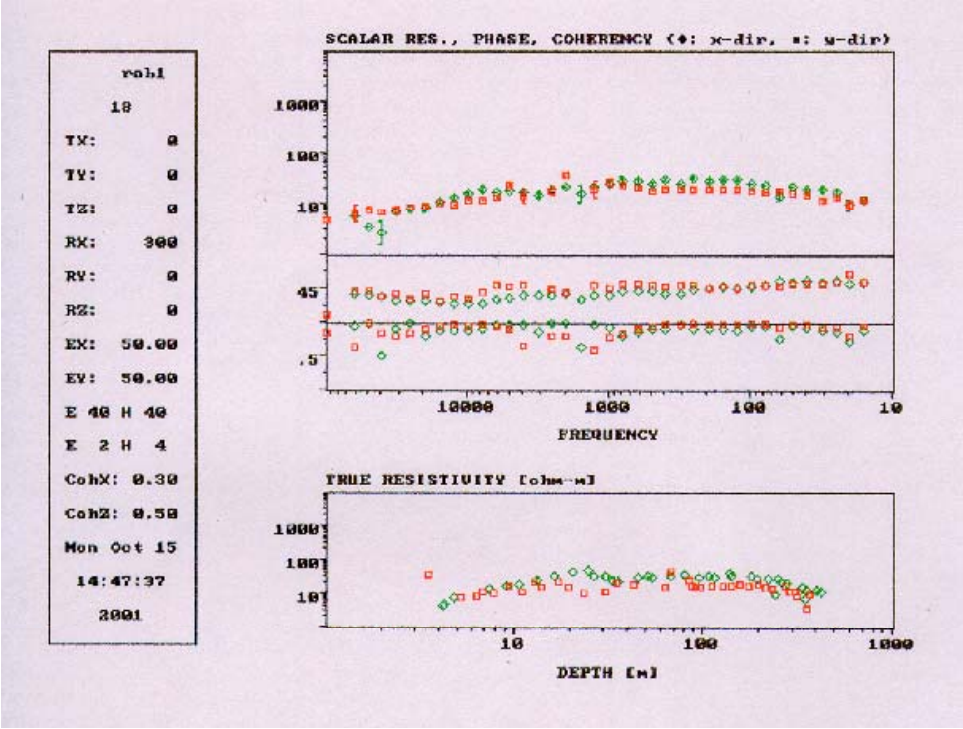
rohl
18
TX: 0
TY: 0
TZ: 0
RX: 300
RY: 0
RZ: 0
EX: 50.00
EY: 50.00
E 40 H 40
E 2 H 4
CohX: 0.30
CohZ: 0.50
Mon Oct 15
14:47:37
2001
SCALAR RES., PHASE, COHERENCY (♦: x-dir, ▪: y-dir)
1000
100
10
45
.5
10000
1000
100
10
FREQUENCY
TRUE RESISTIVITY [ohm-m]
1000
100
10
10
100
1000
DEPTH [m]

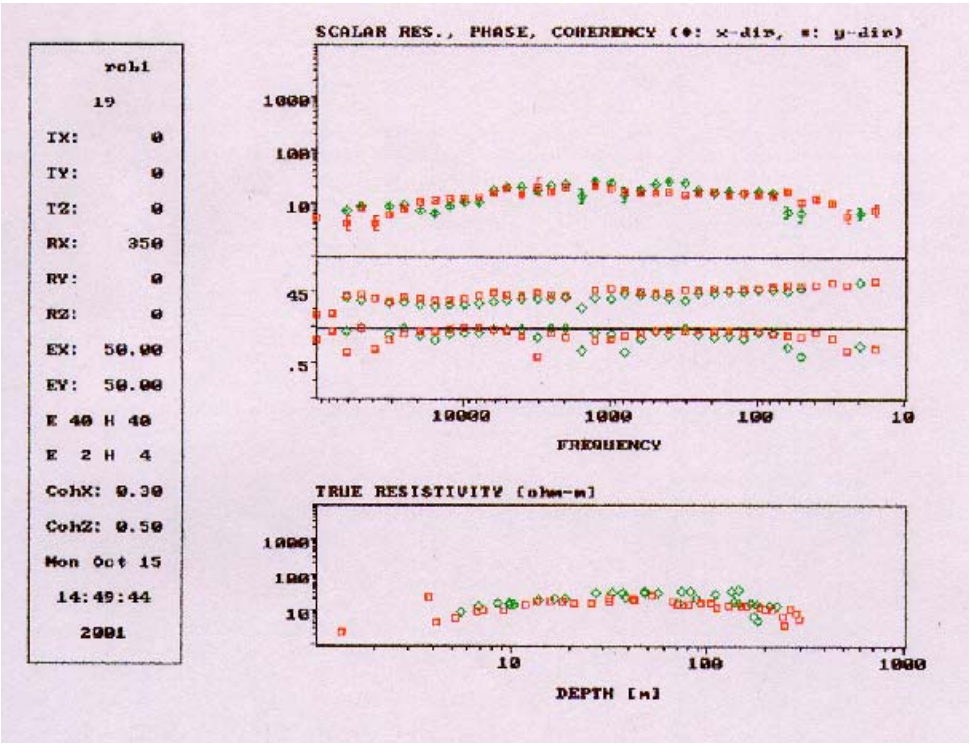
rohl
19
TX: 0
TY: 0
TZ: 0
RX: 350
RY: 0
RZ: 0
EX: 50.00
EY: 50.00
E 40 H 40
E 2 H 4
CohX: 0.30
CohZ: 0.50
Mon Oct 15
14:49:44
2001
SCALAR RES., PHASE, COHERENCY (♦: x-dir, ▪: y-dir)
1000
100
10
45
.5
10000
1000
100
10
FREQUENCY
TRUE RESISTIVITY [ohm-m]
1000
100
10
10
100
1000
DEPTH [m]

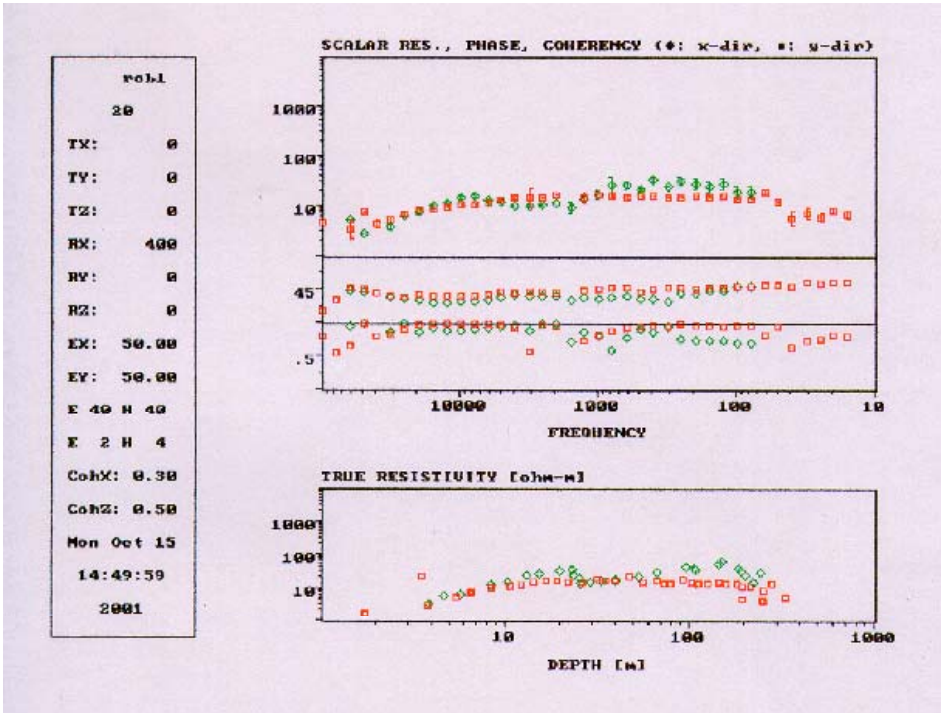
robl
20
TX: 0
TY: 0
TZ: 0
RX: 400
RY: 0
RZ: 0
EX: 50.00
EY: 50.00
E 40 H 40
E 2 H 4
CohX: 0.30
CohZ: 0.50
Mon Oct 15
14:49:59
2001
SCALAR RES., PHASE, COHERENCY (+: x-dir, *: y-dir)
1000
100
10
45
.5
10000
1000
100
10
FREQUENCY
TRUE RESISTIVITY [ohm-m]
1000
100
10
10
100
1000
DEPTH [m]

11 APPENDIX II—TEM soundings

This appendix shows TEM sounding data and 1-D inversion results for the 8 sounding sites. Soundings 1 through 4 are on the north-south line, Line 1. Sounding 1 is the northmost sounding site. Soundings 5 through 8 are on the east to west line, Line 2. Sounding 5 is on the east end of the line where it intersects Line 1.

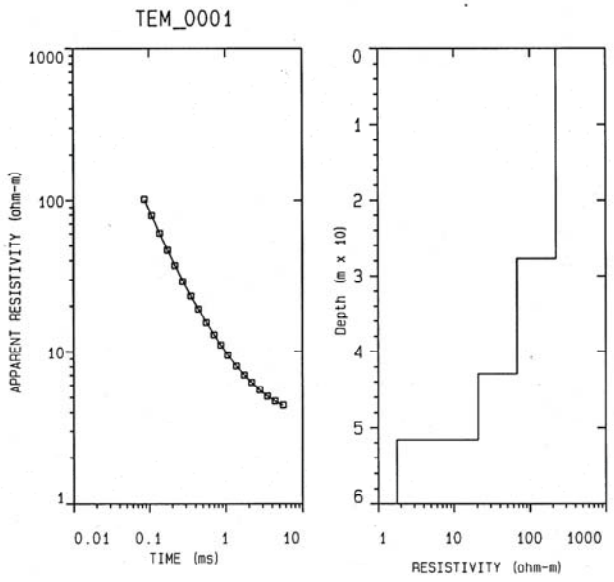

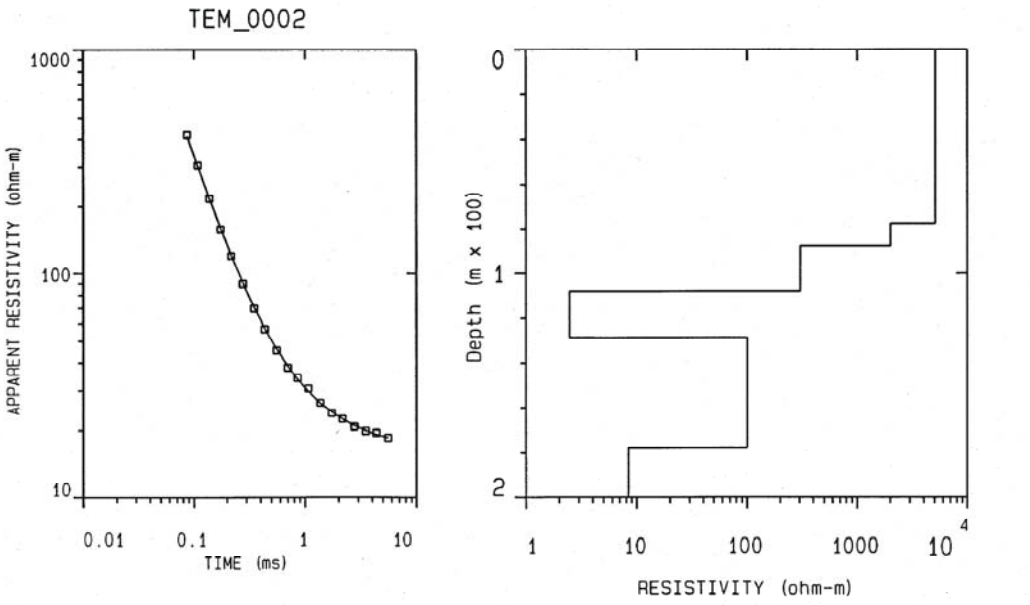

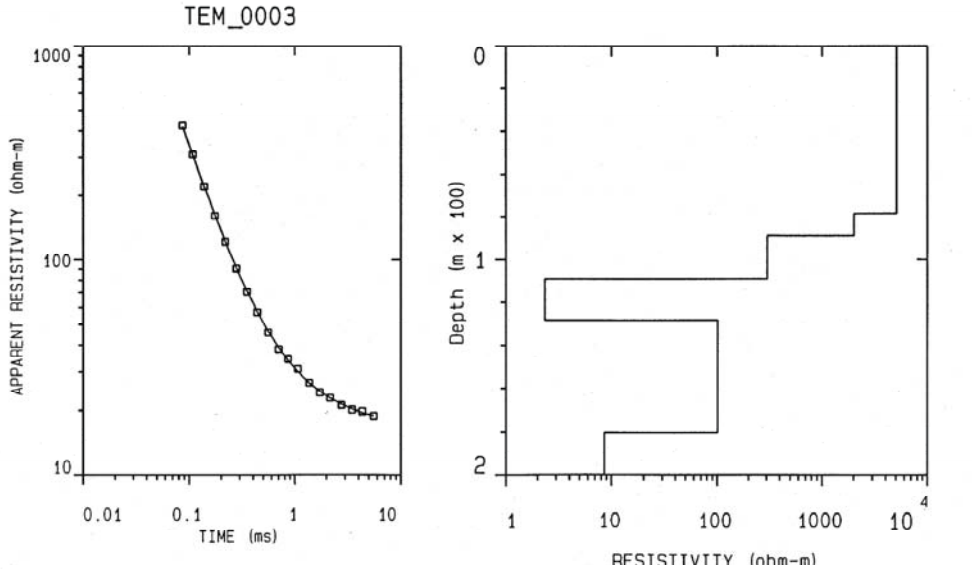
TEM_0003
APPARENT RESISTIVITY (ohm-m)
1000
100
10
0.01
0.1
1
10
TIME (ms)
Depth (m x 100)
0
1
2
1
10
100
1000
10 4
RESISTIVITY (ohm-m)

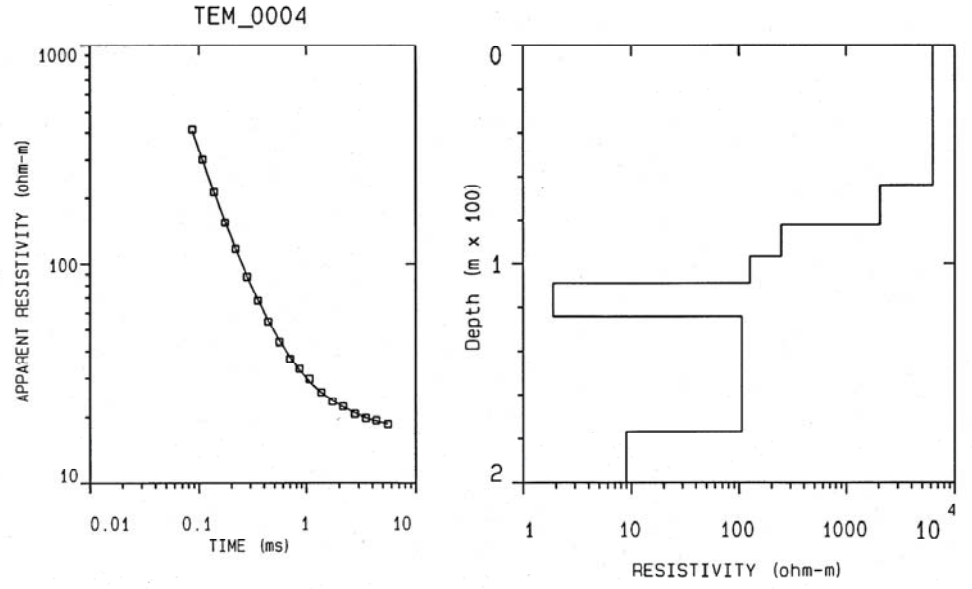
TEM_0004
APPARENT RESISTIVITY (ohm-m)
1000
100
10
0.01
0.1
1
10
TIME (ms)
Depth (m x 100)
0
1
2
1
10
100
1000
10 4
RESISTIVITY (ohm-m)

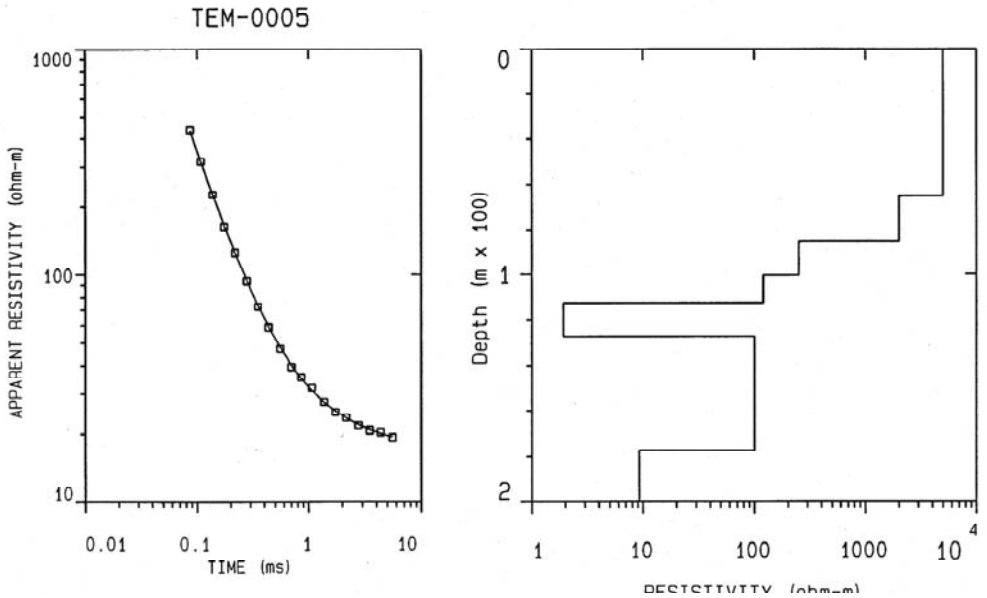
TEM-0005
APPARENT RESISTIVITY (ohm-m)
1000
100
10
0.01
0.1
1
10
TIME (ms)
Depth (m x 100)
0
1
2
1
10
100
1000
10^4

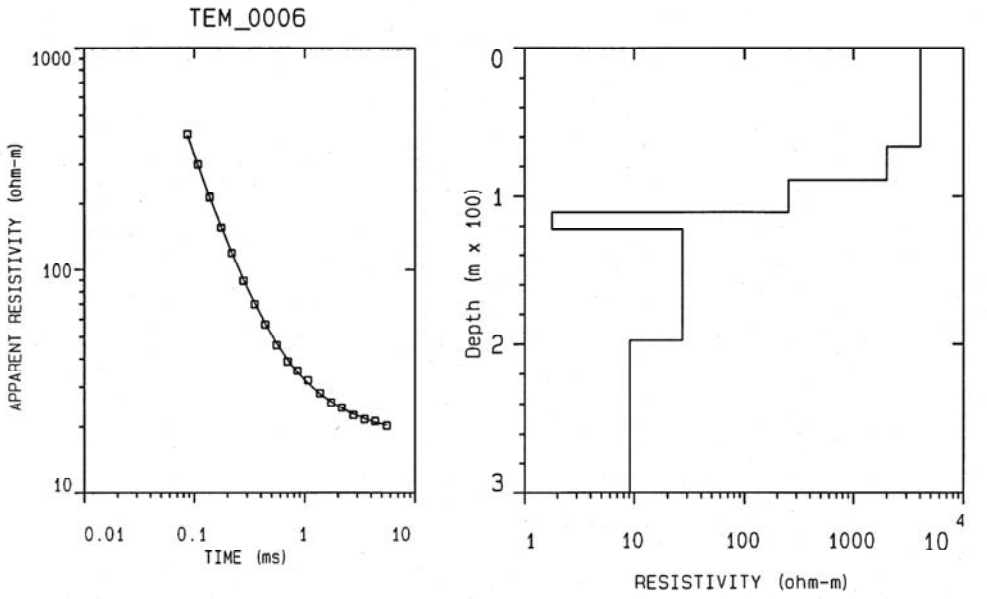
TEM_0006
APPARENT RESISTIVITY (ohm-m)
1000
100
10
0.01
0.1
1
10
TIME (ms)
Depth (m x 100)
0
1
2
3
1
10
100
1000
10^4
RESISTIVITY (ohm-m)

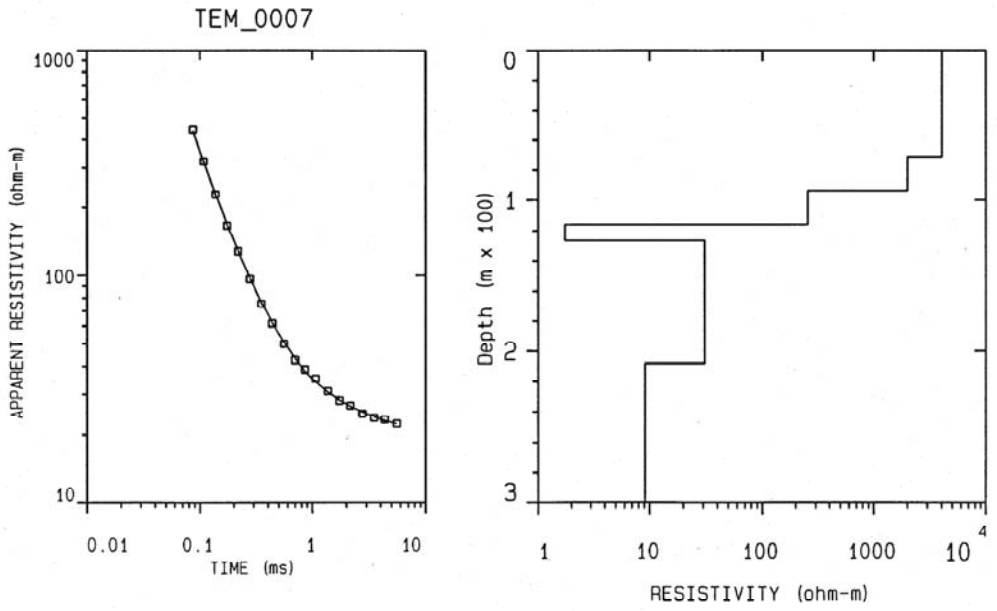
TEM_0007
APPARENT RESISTIVITY (ohm-m)
1000
100
10
0.01
0.1
1
10
TIME (ms)
Depth (m x 100)
0
1
2
3
1
10
100
1000
10 4
RESISTIVITY (ohm-m)

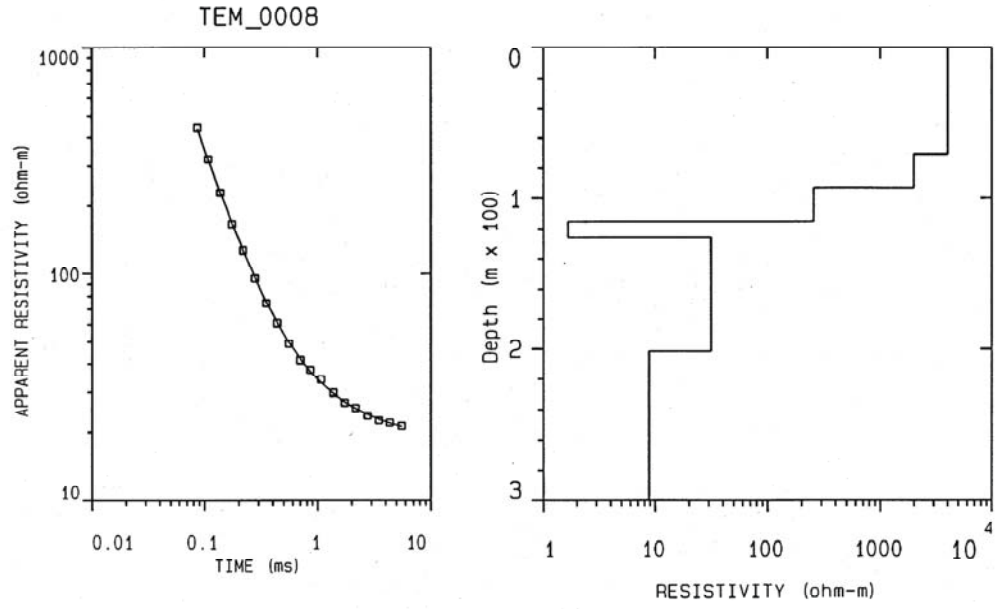
TEM_0008
APPARENT RESISTIVITY (ohm-m)
1000
100
10
0.01
0.1
1
10
TIME (ms)
Depth (m x 100)
0
1
2
3
1
10
100
1000
10 4
RESISTIVITY (ohm-m)